Journal of Radioanalytical and Nuclear Chemistry (2019) 321:1–30
https://doi.org/10.1007/s10967-019-06559-w

Advances on identification and animated simulations of radioactivity risk levels after Fukushima Nuclear Power Plant accident (with a data bank): A Critical Review

Fatih Külahcı[1] · Ahmet Bilici[1,2]

Received: 21 October 2018 / Published online: 13 May 2019

Abstract

This review study has been based on two main foundations as advances on the attainment of the risk radioactive fallouts levels, and the applications of methods for risk assessment to actual data and visual results, which are based on a 3-year study. A risk analysis model is developed with the animated simulations including the isotope distribution based on soil activity data, ^{131}I measured at 19 stations after the Fukushima accident. Probability distribution functions of the risk levels are obtained in addition to the probability of occurrence (risk) and the probability of non-occurrence (reliability) of the activity risks concerning ^{131}I. The results are used for prediction of 60-day radioactive fallout subsequence and animated (.mp4) through simulations.

Electronic supplementary material The online version of this article (https://doi.org/10.1007/s10967-019-06559-w) contains supplementary material, which is available to authorized users.

✉ Fatih Külahcı
fatihkulahci@firat.edu.tr

[1] Science Faculty, Nuclear Physics Division, Physics Department, Fırat University, 23119 Elazig, Turkey

[2] Vocational School of Health Service, Department of Opticianry, Bartin University, Bartin, Turkey

Graphical abstract

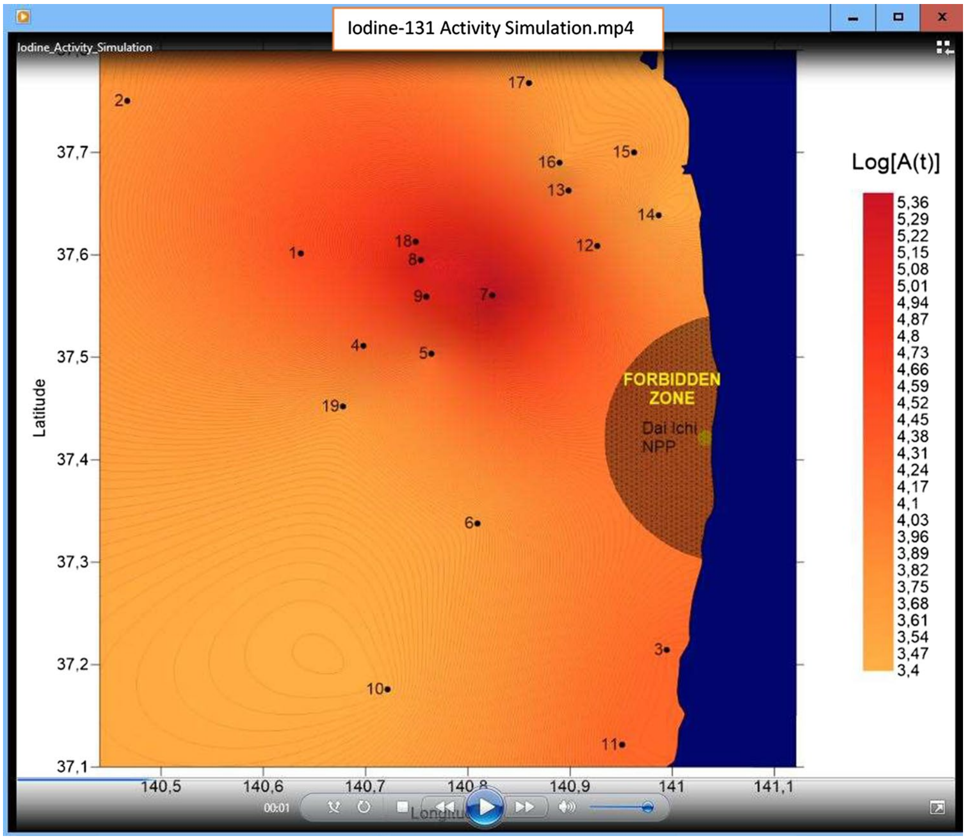

Keywords Spatial modelling prediction · Kriging · Radionuclide migration · Long-range transport · Radioactive fallout · Risk assessment

List of symbols

λ	Radioactive decay constant
$t_{1/2}$	Radioactive half-life
t	Time parameter
N_0	Number of initial radioactive nuclei
$N(t)$	Number of radioactive nuclei at time t
$N_r(t)$	The number of nuclei at time t of rth radioactive nucleus
$N_n(t)$	Number of nuclide in time t of stable nuclide
A_0	The initial activity
$A(t)$	Activity in time t
x_i	ith independent parameter
$f(x_i)$	ith dependent parameter
$g(x)$	Theoretical curve
ε_i	ith error
E	Square of the sum of errors
a_i	ith coefficient
x_0	Prediction point
$w_i(x_0)$	Weight value indicating the contribution from the ith station for the prediction point
G	Confidence
R	Risk
s	Sum of all cases
g	Probability/event of non-occurrence
r	Probability/event of occurrence
m	Rank
g_b	Probability of non-occurrence for biggest activity value
m_b	The rank for biggest activity value
n	The number of all activity events
A	Activity event
$P(A)$	Probability of occurrence of event A
A_s	Small activity value event
A_b	Great activity value event
α	Scale parameter for Weibull distribution
β	Shape parameter for Weibull distribution
μ	Location parameters for the lognormal and generalized extreme-value distributions
σ	Scale parameter for the lognormal and generalized extreme-value distributions

k	Shape parameter for generalized extreme-value distribution
$f(x\|k, \mu, \sigma)$	Generalized extreme-value distribution function
$F(x\|k, \mu, \sigma)$	Generalized extreme-value cumulative distribution function
g_{gev}	Probability of non-occurrence for generalized extreme-value distribution
r_{gev}	Probability of occurrence for generalized extreme-value distribution

Introduction

Three Mile Island, Chernobyl, and the Fukushima Dai-Ichi nuclear power plant (FDNPP) accidents took place in March 2011, which are important spots in the history of nuclear power accidents. The tsunami waves after the Tohoku earthquake of 8.9 magnitude broke out on the Honshu Island openings on March 11, 2011 at 14:46, resulting in the FDNPP reactor accident. After the earthquake, the diesel generators started to supply power to the to the electricity circuit that was automatically interrupted. Tsunami ripples caused electric supply to cease within a short time. Because of energy loss, the cooling systems were shut down and then the explosions came to fruition. Meanwhile, radioactive caesium and iodine emissions were mixed in the atmosphere. Subsequent to the occurrence of the accident, a safety circle of 20 km was built. Approximately 80,000 people were removed from this area, and any non-authorized person was not taken to the area. In this study, radioactive fallout calculations are performed by taking into account the restriction region [1–7]. The FDNPP accident was classified as level 7 according to the International Nuclear Events Scale (INES) system [1, 8]. After FDNPPA, the effects of radioactive fallout were measured in many places. According to these measurements, almost all of the American and Asian continents were affected by the accident. In some East Asian countries, the dose levels have reached, in places, the limit values announced by the IAEA [9–21]. Other studies have shown how the accident affected western and northern western regions of Europe [22–25].

The follow-up radionuclides traces on ecosystems is crucial both scientifically and in terms of viability in the relevant ecosystem [26–28]. Radionuclide distribution affects not only humans, but also marine and terrestrial ecosystems [29]. The major reactor accident radionuclides, ^{137}Cs and ^{129}I, have significant effects on air quality, and to see these effects, researchers have recently started to work on climate models [30–42]. Concurrently, new models [43–46], simulation techniques [41, 47–49] and risk analyses [50–70] are continuously employed for how to remove radioactive fallout products from nature [71]. In such studies, global radionuclides transport mechanisms [4, 72–79] are generally observed using systems of differential equations or statistical modeling approaches [80–83].

After the FDNPPA accident in March 2011, a serious radio-nuclear wave was delivered to the neighborhood. It is not possible to instantly monitor (or observe) all of the data related to the radionuclides emitted to the environment, which cause to data deficiencies that are generally a problem for similar investigations. For this reason, atmospheric dispersion model [84–86] approaches are used to partially compensate for errors in calculations [87]. The total amount of ^{131}I released to the atmosphere after the FDNPP accident was measured as 120-380 PBq [10, 83, 87–97] following the accident, the ^{131}I was first detected in Fukuoka, 1000 km from the FDNPP, 3 days after the accident [16]. Detection of short half-life ^{131}I is important for short exposures. It causes global atmospheric oscillations despite short half-lives [98]. It was detected in Vietnam at 4500 km from Japan between March 27 and April 22 after the first detection [99]. On March 28, the presence of ^{131}I was identified in the Republic of Korea about 1000 km from Japan [100]. On the other hand, the precipitation behavior of Iodine's longer half-life isotope ^{129}I (1.6×10^7 years) emissions were characterized as a result of detailed studies [101]. Since, ^{131}I has a relatively short half-life, it is, therefore, a difficult radionuclide for such long-term monitoring works. This makes it difficult to obtain its transport characterizations. For all these reasons, it was decided to work on ^{131}I, and moving visual simulations were also made for an effective methodology leading to transport risk analysis and activity intensity maps. Five years after the accident (in 2016), a study by Arai [102] detected the presence of FDNPP-originated radioactive particles in the natural environment. Similar findings were obtained through simulation program developments [21, 103–106]. This shows the importance of the simulation studies in large-scale areal researches. For example, by simulating Fukushima-derived radioactive fallout, it was possible to obtain meaningful conclusions about the behavior of radionuclides in the oceans [107]. As a result of various works on combining experimental and theoretical studies, the distribution of radioactive fallout was interpreted successfully [108], and hence, visual changes were easily visible. Apart from simulations, activity density maps also provide large-scale analysis [109].

After Fukushima NPPA, the presence of ^{131}I in Europe has also been identified. The presence of these traces shows that the radioactive clouds move horizontally along with the vertical movement towards the troposphere. This horizontal movement causes ^{131}I to be present in the air near the ground level [110]. Especially, after the Chernobyl accident, it is possible to see this in the global assessments studies of radioactive contamination [54, 83, 111–115]. It is far more difficult to remove ^{131}I from the water environment by conventional methods such as coagulation, flocculation and sedimentation methods than ^{134}C and ^{137}Cs. Its short half-life ($t_{1/2} = 8.05$ days) makes its detection difficult, but increases the importance of its analysis, because it is an important pollutant [95]. After FDNPP, significant quantities of ^{131}I, ^{134}Cs, and ^{137}Cs were found to be deposited on the soil surface in Japan on March 21-23, 2011 due to rains in Japan [10–15, 116–119]. Again, according to Unno et al. [10], Xu et al. [11–13], Yamaguchi et al. [14, 15] these radionuclides originating from the radioactive fallout had accumulated on the soil surface [120] and adhered to the dust particles resulting from agricultural activities [121] and remixed to the atmosphere. Indeed, the effects of climate change were as a result of anthropogenic radionuclides mixing into the atmosphere in the Asian dust-collecting zone, and radionuclides adhering to dust particles fold into long distances by mixing into the atmosphere [122]. These transports were examined spatio-temporally and the transport characteristics of radionuclides were determined over time [123–125].

The Fukushima accident brought to light the issues of public health, economy, international relations and the energy policies re-examination, the release of radioactivity and its distribution [126]. It is scientifically important to see the size of the fallout formed by the radionuclides, which radiate to the atmosphere during and after the FDNPPA. In addition to the long half-life radionuclide exposure that occurs immediately after the reactor accident, short exposure is also important. In this study, the risks and risk scenarios, pollutant and transport characteristics and partially health, sociological and psychological effects of radioactive fallout and especially short half-life ^{131}I environmental exposures are reviewed, and a new "moving simulation method" is proposed using the spatial analysis method [127]. With the proposed simulation study, it is possible to visualize the behaviours and characteristics of the radioactive fallout clouds. In this study, the proposed simulation method was based on the Kriging methodology [128] and semivariogram concepts [129], which have an important place in geostatistics methods [130, 131]. Somewhat important updates were made on this method and concept and they are used sometimes in different disciplines [127, 132–149].

Risk analysis [150–154], modelling and simulation studies [155–161] are important in determining the effects of radioactive fallouts. Such studies could make important predictions on the study area at that or for a further time. These estimates are also important for the development of nuclear waste scenarios [162–165]. The creation of these scenarios is important for society and environmental health [166–168]. In this study, previous monitoring, simulation, and modeling studies are evaluated from a broad perspective and motion activity distribution simulations and activity risk analysis for ^{131}I after FDNPPA is obtained. This article contains two parts, review part (radionuclides and the risk assessments of the radioavtive fallouts, items 1–4) and model simulation part (simulation and risk assessment for the Fukushima Dai-Ichi accident area, item 5). Moreover, significant approaches and interpretations are obtained on the radioactive fallout risk levels. The effects of radioactive fallout in Fukushima are determined for ^{131}I radionuclide. Both risk analysis and simulation studies are performed to predict the characterization and transport of the radioactive fallout prospectively. The data for the risk analysis is obtained from Japan Ministry of Education, Culture, Sports, Science, and Technology (MEXT). The probability of ^{131}I contamination (risk) formation up to a distance of 60 km from the site of the reactor accident and the probability of non-occurrence of contamination (confidence) are determined for the next 60 days. The simulation studies for risk and probability calculations in addition to the characterization of contamination are obtained as .mp4 files in motion. These animated simulations provide considerable convenience in visualizing how the contamination evolution takes place by time. Radioactive particles transport simulation is important especially for the characterization of radioactive fallouts and for future predictions.

^{131}Iodine

Despite the short half-life of ^{131}I following FDNPP accident, it can be said that global transport [169–171] is serious. As a matter of fact, it is estimated that 11,000 km away in the accident region in the USA [172–174], in the Pacific Ocean [175, 176], in Canada [177], in Greece [22, 178], in France [179, 180] and in the other regions of Europa [23, 181–184]. ^{131}I reached Europe only 7 days after the accident [23, 185–188]. ^{131}I and some other fission products were detected at distances from the troposphere layer [189–191] whereas, Matsui [192] theoretically calculated ^{131}I based on the existing information from nuclear reactions and activity densities in the environment.

Radionuclides such as ^{95}Zr, ^{103,106}Ru, and ^{140}Ba are detected in the Chernobyl reactor accident, and they differ from those in the Fukushima accident. In Fukushima, it is shown that the ones emitting terrestrial broadness are inert gases and volatile radionuclides of which ^{131}I occupies an important place [19, 193, 194]. Some of the most effective physical mechanisms play a great role in the spread of ^{131}I, which are wind and rain [195]. In this study, ^{131}I data for the application of methodologies are taken by MEXT 3 days after the accident. In this period, MEXT reported that the global air circulation was not ineffective [196].

Removal of ^{131}I from the water environment by coagulation-flocculation-sedimentation methods did not yield the desired results. On the other hand, ^{134}Cs and ^{137}Cs coagulation could be removed in the same medium [197]. Water purification and filtration systems are recommended for removal of radionuclides from drinking water [197, 198]. "Nano-metallic Ca/PO_4″ has been proposed to remove the above fission products from the surrounding environment or to reduce their mobile capability. This material was used by the ball milling method and reduced the mobilization of the fission products in the soil by about 56% [199]. With the development of these new techniques, it is thought that serious progress can be achieved in the reduction of possible cancer cases [200].

Approximately 80% of ^{131}I can be stopped at soil depths of 4-6 cm [201, 202]. Apart from soil-depth analyses [203–207], ^{131}I determination analyses were performed on a large scale on the soil surface [208, 209]. The transport characterization of ^{131}I is also modeled, which then adheres to the dust particles [14, 80, 210]. This progression and distribution of ^{131}I in the soil were modeled through numerical simulations [211]. In the atmospheric distribution [92, 212]; the Bayesian method [213], the Monte Carlo technique [214, 215], the time series analysis [12, 216], the mathematical modeling [217, 218] and in particular the inverse modeling methods [43, 55, 80–82, 84, 91, 92, 212, 213, 219–231] have recently become quite popular at atmospheric contaminants [232–234] and fallout studies [230, 235]. These modeling techniques have brought a different perspective to the characterization of the atmospheric ^{131}I transport and some other fission products [90, 92, 93, 219, 226, 236–240]. ^{131}I and some other fission products have been also reported as significant contamination indicators in the aquatic environments [13, 241, 242]. The environmental contamination of ^{131}I necessitated the investigation of its effects on the lives of the living creatures [15, 243–250]. Examining the effects of her breastmilk, it was a pleasing situation that no feared results occurred [10, 251]. Apart from cancer research on thyroid [252], improvements and innovations in the field of engineering are also noteworthy. Utilizing the accumulation of ^{131}I on thyroid glands [253], ultra-sensitive biomonitors were also developed [254]. In a similar vein, from the thesis that "radioactive nuclei could be seen with the naked eye, could be controlled more easily"; high-resolution molecular sensors have been proposed [255].

The answer given by the creature that received the radiation dose is very important [256]. The decontamination map generated as a result of these responses is determined by the atmospheric monitoring results and the dose of radiation calculated from the stations at the first period of the FDNPPA. The decontamination protocol advocates individuals' reassessment, who wish to live in these areas according to their individual doses and it is an improvement on the response of living things to the dose–response relationship [257, 258]. On the other hand, radiological investigations continue to predict the amount of ^{131}I activity, which is difficult to detect using experimental methods, unlike the theoretical methodologies in this study [259].

Radioactive fallout risk analyses and risk assessments

Radioactive fallouts risk analysis and studies on nuclear scenarios began in 1992 by Harvey et al. [260], which found practical applications. According to the studies conducted 4–5 years after the Chernobyl accident on the Chelyabinsk-65 population, in human organs and tissues ^{238}Pu and ^{239,240}Pu were found three-four times higher than global levels. These results also brought serious health problems like cancer [261–267]. In 2001, lessons on the radioactive fallout health effects began to be taught [52]. It has led to the development of interesting computational tools such as web-based and GIS-based on the determination of the risk levels of nuclear weapons trials radioactive fallout. The computational techniques development revealed the necessity for eliminating statistical errors and uncertainties [268]. The environmental and health anomalies that appeared even after 50 years of radioactive exposure seem to occupy the present world of science [269–272]. Indeed, research on radioactive clouds global effects after major reactor accidents is an important step in determining risk levels [83, 111–113, 273, 274]. Uncontrolled reactor discharges, which cause to local health and environmental effects, also disrupt atmospheric C-14 equilibrium while Chernobyl's effects are still discussed [275], although not globally as Chernobyl [276].

Fukushima risk analyses and risk assessments

After the Fukushima Dai-Ichi reactor accident, risk scenarios were established by considering radionuclide fallouts around the area, posing possible health risks for living [3, 277–279]. Apart from these scenarios, the radioactive fallout products' effects on the food sector [280], other than the risks posed to living beings directly in the marine [281, 282] and terrestrial environments, have been studied in a broad perspective [283–285]. Communication tools [286, 287] were developed to present Fukushima risk analysis [288–291] and risk assessment results [238, 292–300]. On the other hand, important proposals were made on re-observing the construction of reactors and central buildings on the grounds that nuclear reactors known to be very resistant to earthquakes and they were influenced by tsunami [154, 301–305]. FDNPPA, the sociological and psychological effects of the incident have been on the agenda many times [305–314]. Particularly, health and more especially the cancer risk and its effects on humans have been one of the serious research topics [237, 238, 277, 315–323]. In the time frame from the 2011, Fukushima reactor accident to the present day, risk assessments on the occurrence of reactor accidents and the distribution of radioactive fallouts [9, 83, 99, 111–113, 227, 324–340] and determination of the risk of the effects of reactor accidents on health were the main research topics [200, 214, 341–364].

Simulation of radioactive fallout

Ability to simulate the radioactive fallouts propagation has opened a new door in this era [365]. The first simulation study is identified for iodine that belongs to Sorensen [366]. Later, the Japan Atomic Energy Agency obtained dynamic simulations for rice paddy fields and ^{137}Cs deposited in rice [367, 368]. Simulation studies have been proposed as a result of the convenience for the spread of radioactive fallouts' interpretation, and simulation studies for some other hazardous materials [369, 370]. Radioactive fallouts were detected in fallout decay simulations that caused mutation in some flower pollen [371]. For instance, the detection of the ^{90}Sr and ^{137}Cs fallout products effects on soybean plants play directly a role in the development of the plant physiological development, which is another important consequence [372]. In 2008, Macedonio et al. [373] simulated the fallout, which was formed as a result of the volcanic activity of Vesuvius. Finally, motionless simulations of the reactor accident of Chernobyl were obtained [112]. It is also obtained in this study the propagation of the Fukushima reactor accident product ^{131}I as moving simulations for a 60-day forward-looking estimation.

On simulation of Fukushima radioactive fallout

Simulation models have been used quite often recently for prospectively predicting the characterization of the amount or behavior of the variables concerned. Simulation techniques [85, 86, 374, 375] applicable from microscale to macro scales include new interpretations [376, 377] and new scientific advances [239, 378–382]. The destructive tsunami effects in the Fukushima reactor caused damage on the accident scenarios as little as possible from similar accidents [383]. In addition, after the reactor accident, alternative solutions to the problems that occurred in electricity generation and related problems came to mind [384] and in parallel with these workings, simulation studies on ^{134}Cs and ^{137}Cs radionuclides were also made [385–389].

Two-dimensional radioactivity distribution maps were obtained by using numerical simulation techniques for the characterization of radioactive water emitted from FDNPP [156, 215, 390]. These maps give the researcher detailed information about the variable studied in large-scale areas. Takemura et al. [157], Danielache et al. [159] and Behrens et al. [158] modeled global atmospheric radionuclide transport by performing numerical analysis on a global scale. After the Fukushima reactor accident, the radionuclides radiated to atmosphere travel far distances [391] over the ocean and through ocean currents [160, 161, 392–396]. Radioactive particles are under the influence of meteorological variables when transported at these distances [397]. As a result of atmospheric transport, fission products that land on the ground can contaminate groundwater [89].

As mentioned above, the findings obtained by simulating the reactor to investigate the causes of the explosion in the Fukushima reactor and the radioactive fallout are bound to provide important clues for controlling similar accidents in the future [398–405].

Real-time theoretical and practical researches for simulation, risk analysis and modeling of radioactive fallout

FDNPP was established near the Okuma Village in the Futaba district of Fukushima Prefecture in Japan and entered into operation in the 1970s as the first nuclear energy reactors generation. This plant was then transformed into a second-generation nuclear power plant with improvements. The plant has six boiling water reactors operated by the Tokyo Electric Power Company (TEPCO) [2, 8, 406].

In this research, since the risk analysis of ^{131}I radionuclide is studied, first, the activity value at any time should be known in each station. Since, the measurements taken by MEXT are not synchronous, it is necessary to obtain the activity curves of the short-lived ^{131}I in each station. For this, whenever the least squares method application to measurements taken from each station, an activity curve can be obtained for each station. Theoretically, once the concurrent activity values are obtained, risk analysis can be performed according to the position. After FDNPPA, soil ^{131}I activity measurements from 19 stations are taken by MEXT [196]. ^{131}I was first discovered in nuclear weapons tests, and this radioisotope is a dangerous radionuclide in NPP accidents. The ^{131}I radioisotope turns into a stable nucleus of ^{131}Xe after negative beta decay and gamma emissions [407, 408]. Information on the latitude, longitude and FDNPP distances of measurement stations are given in Table 1 [196].

Theory

Least squares method

Gauss (1795) originally proposed the least squares method and in 1801, and used this method to determine the orbit of the Ceres asteroid. This method was published in 1809 as the second edition of Gauss' collective works [409]. The least squares method is a standard regression method [410–412],

Table 1 Some information for the stations where the measurements are taken

Station no.	Distance to the plant (km)	Latitude	Longitude	Station name
1	40	37,601444	140,63667	Date, Kawamata Town Yamakiya
2	62	37,750472	140,46686	Fukushima, Sugitsuma Town
3	23	37,214403	140,99467	Futaba, Hirono Town Shimokitaba
4	31	37,511156	140,69791	Futaba, Katsurao Village Kaminogawa
5	25	37,503417	140,76447	Futaba, Katsurao Village
6	22	37,337889	140,80949	Futaba, Kawauchi Village Kamikawauchi
7	24	37,56055	140,82388	Futaba, Namie Town Akougi Kunugidaira
8	31	37,595	140,75402	Futaba, Namie Town Akougi Teshichiro
9	29	37,559156	140,75935	Futaba, Namie Town Shimotsushima Kayabuka
10	39	37,175842	140,72152	Iwaki, Miwa Town Saiso
11	34	37,121783	140,95107	Iwaki, Yotsukura Town
12	23	37,608722	140,92675	Minami Soma, Haramachi Ward Baba
13	29	37,662889	140,89856	Minami Soma, Haramachi Ward Ohara Daihata
14	24	37,638739	140,98684	Minami Soma, Haramachi Ward Takami town
15	32	37,70015	140,96265	Minami Soma, Kashima Ward Terauchi Motoyashiki
16	32	37,690103	140,88981	Minami Soma, Kashima ward Jisabara Aza Kamabai
17	41	37,767864	140,8599	Soma, Yamakami Kaminamik
18	33	37,612803	140,74911	Soma, Iitate Village Nagadoro
19	32	37,451964	140,6779	Tamura, Tokiwa Town Yamane

which is used to write the mathematical relationship between two physical quantities that change in relation with each other.

Measurements taken from some stations by MEXT were not simultaneous. This is an obstacle for simulations and predictions. For this reason, the least squares method (LSM) is recommended for data optimization. The radioactivity values measured at stations in the LSM were determined at equal time intervals. The mathematics of the methodology can be summarized as follows:

In a study, let $g(x)$ be a fitted model curve to the scatter diagram from pairs of $x_i - f_i$ (x; independent variable, f; dependent variable). Here, it is expected that any x_i value corresponds to the values of f_i and $g(x_i)$. The difference between them;

$$\varepsilon_i = (g(x_i) - f_i) \tag{1}$$

gives the *ith* error. For every x_i, this error can be positive or negative in the calculation of errors sum, so in order to avoid zero sum each error is squared. Sum of squares errors is given by,

$$E = \sum_{i=1}^{n} \varepsilon_i^2 = \sum_{i=1}^{n} \left(g(x_i) - f_i\right)^2 \tag{2}$$

Suppose that the function $g(x)$ depends on x and expressed in terms of coefficients a_i ($1 \leq i \leq n$). Let us choose a function $g(x)$ which yields the following condition.

$$\frac{\partial E}{\partial a_i} = 0 \tag{3}$$

If Eq. (3) is combined with Eq. (2), then one can obtain,

$$\sum_{j=1}^{n} g(x_j)\frac{\partial g(x_j)}{\partial a_i} = \sum_{j=1}^{n} f_j \frac{\partial g(x_j)}{\partial a_i} \tag{4}$$

If i-equation systems are solved as given by equation Eq. (4) and have i-variables, coefficients a_i should be solved for the best fit [411, 413]. Finally, the least squares method can be used to obtain synchronous activity curves, if samples are taken at different times in different stations. Thus, in calculations optimizations are provided.

Least squares method results

The time between the receipt of the ^{131}I measurements and the date of the reactor accident was taken as parameter t. If the sought dependent parameter is activity, then it is necessary to obtain an exponential curve as in Eq. (5), according to the classical radioactive decay law.

$$A(t) = A_0 e^{-\lambda t} \tag{5}$$

If natural logarithms are applied on both sides of Eq. (5), a linear equation is obtained as in Eq. (6).

$$\ln (A(t)) = \ln \left(A_0\right) - \lambda t \tag{6}$$

If the equation $g(x)$ in Eq. (4) is written as in Eq. (7), then one can obtain,

$$g(x) = g(t) = \ln(A(t)) = \ln(A_0) - \lambda t \tag{7}$$

Equation (4) can be rewritten as follows,

$$\sum_{j=1}^{n} g(t_j)\frac{\partial g(t_j)}{\partial a_i} = \sum_{j=1}^{n} f_j \frac{\partial g(t_j)}{\partial a_i} \tag{8}$$

This is a linear form and has two coefficients as,

$$a_1 = \lambda \quad \text{and} \quad a_2 = \ln(A_0) \tag{9}$$

After differential operations, Eq. (8) becomes a system of two linear equations with two unknowns (λ and $\ln(A_0)$), in the form of Eq. (10). With the aid of MATLAB® software program, the system of Eq. (10) is solved to yield activity values given in Table 2 and the other tables in Appendix A (supplementary material) and the coefficients a_1 and a_2 are obtained as in Table 3 for each station. This table shows the station numbers in the first column, the decay constant (λ) in the second column, the initial activity value ($t=0$) in the third column and the square of the correlation coefficients (R^2) of the curves obtained with these constants in the fourth column.

$$\begin{aligned} \ln(A_0)\sum_{j=1}^{n} t_j^2 + \lambda \sum_{j=1}^{n} t_j &= -\sum_{j=1}^{n} f_j t_j \\ \ln(A_0)\sum_{j=1}^{n} t_j + \lambda n &= -\sum_{j=1}^{n} f_j \end{aligned} \tag{10}$$

The half-life of ^{131}I is $t_{1/2} = 193.68 \pm 0.216$ h. Again, the decay constant in hours is theoretically,

$$\lambda \cong 0.00357883 \text{ h}^{-1} \tag{11}$$

The differences in activity values in Table 3 are thought to be due to geographical and meteorological situations, which indicate that the activity is stochastic relative to the position. Due to randomness, statistical considerations and

Table 2 Activity values measured and calculated versus time for station 1. For example, here "337th term" describes the 337 h after the reactor accident

Time (h)	Experimental (measured) activity (Bq/kg)	Theoretical (calculated) activity (Bq/kg)	Time (h)	Experimental (measured) activity (Bq/kg)	Theoretical (calculated) activity (Bq/kg)
337th	73,000	79,698.910	1171st	2400	3011.989
364th	49,000	71,679.840	1196th	2200	2730.294
403rd	65,000	61,499.650	1219th	2600	2494.463
427th	63,000	55,967.320	1243nd	2800	2270.069
452nd	71,000	50,733.010	1267th	2400	2065.860
476th	59,000	46,169.220	1292nd	2600	1872.652
500th	54,000	42,015.980	1315th	2000	1710.900
525th	54,000	38,086.460	1339th	2200	1556.993
572nd	6600	31,666.510	1367th	1700	1394.844
596th	31,000	28,817.880	1387th	1900	1289.468
621st	41,000	26,122.710	1411st	1700	1173.471
644th	39,000	23,866.340	1435st	1100	1067.909
668th	27,000	21,719.400	1459st	1100	971.843
715th	14,000	18,058.320	1483rd	220	884.419
740th	22,000	16,369.430	1507th	640	804.859
790th	15,000	13,450.730	1531st	1300	732.456
811st	17,000	12,385.820	1556th	1100	663.954
835th	5600	11,271.630	1579th	330	606.605
859th	6000	10,257.670	1604th	400	549.872
883rd	9900	9334.919	1774th	570	282.022
907th	17,000	8495.178	1945th	85	144.079
957th	4600	6980.471	1946th	110	143.514
979th	9100	6402.626	1947th	170	142.951
1004th	4300	5803.825	1947.5th	160	142.671
1051st	3800	4825.517	1948th	180	142.391
1147th	1500	3309.721			

Table 3 Coefficients and correlation coefficients obtained by least squares method

Station	λ (1/h)	A_o (Bq/kg)	R^2
1	0.00392764	299,427.434	0.94188
2	0.00368719	59,981.314	0.92728
3	0.00367660	154,352.189	0.80427
4	0.00351894	123,625.373	0.87599
5	0.00327673	105,136.900	0.89842
6	0.00344032	33,636.099	0.91790
7	0.00340739	1,961,742.037	0.97333
8	0.00388169	1,239,414.465	0.90204
9	0.00350144	671,291.719	0.89085
10	0.00420333	34,583.151	0.88103
11	0.00356767	141,672.615	0.91622
12	0.00376052	104,126.364	0.88164
13	0.00356378	48,055.164	0.90667
14	0.00367816	27,845.916	0.87996
15	0.00340255	37,610.889	0.93641
16	0.00372990	43,316.681	0.89384
17	0.00382736	51,806.960	0.94033
18	0.00351501	64,909.409	0.94780
19	0.00354769	37,852.631	0.90886

calculations should be introduced after this phase. As an example, the experimental (measured) and theoretical (calculated) activity values for Station 1 are given in Table 2. These operations are performed for 19 stations and the theoretical calculations for all other stations are given in Appendix A (supplementary material).

In Table 3, the equation of the curve for Station 1 is.

$$A(t) = 299427.434\,e^{-0.00392764t} \tag{12}$$

The value at the time given by the least squares method in columns three and six is calculated from Eq. (5).

The result of these calculations is shown in Fig. 1, which shows the output of the computer program written in MATLAB® language to obtain the *Activity* = *f*(*t*) graph for station 1. In this figure, the curve in red line is the most suitable one for station 1 as a result of the LSM. The graphs obtained from all other stations are given in Appendix B (supplementary material).

Risk analysis and probability distribution functions (PDFs)

Risk can be defined as the percentage of adverse events occurrences. Herein, it is defined as the process of scaling the risks that radioactive fallout will form and the areal determination, where measurements need to be taken. When a risk is determined for an event, the given data sets are considered individually and the states for each data are calculated.

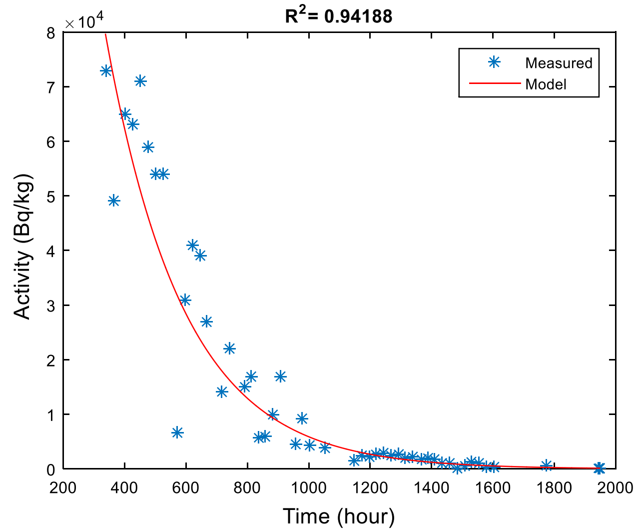

Fig. 1 Measured (experimental) activity values versus time for station 1. The curve on the graph was obtained by the least squares method. (Color figure online)

In this part of the research, risk values are obtained with an experimenter approach. If R denotes the probability of occurrence (i.e., the occurrence of activity) and G denotes the probability of non-occurrence of an event, then the sum of the probability and absence of an event ($G+R$) is always fixed.

$$G + R = s \tag{13}$$

The constant s is the sum of the probability of occurrence and the probability of non-occurrence of ^{131}I fallout. By dividing both sides of Eq. (13) by the constant s, the probability of non-occurrence and probability of occurrence ratios are obtained.

$$g + r = 1 \tag{14}$$

At any given moment, the activity values from a location are sorted from small to big values, and hence, any activity value event (A_b) will itself include small activity events (A_s). One can express this event with A,

$$P(A \le A_b) = P(A \le A_s) + P(A_s < A \le A_b) \tag{15}$$

As the expression in Eq. (15) implies the probability of the given activities will increase steadily to one. This means that the probability functions are cumulative [133, 414–416].

$$g_b = \frac{m_b}{n} \tag{16}$$

where g_b is probability of non-occurrence for biggest activity value, m_b is the rank for biggest activity value, and n is the number of all activity events. However, this is not realistic in practice. The greatest activity for this is not 1, it should be very close to 1. Instead of Eq. (16), it is preferable to write,

$$g_b = \frac{m_b}{n+1} = \frac{n}{n+1} \tag{17}$$

Thus, the bigger active area in Eq. (17) is acceptable. The most general form of Eq. (17) for each rank is given as

$$g = \frac{m}{n+1} \tag{18}$$

And from Eq. (14) one can obtain,

$$r = 1 - g = 1 - \frac{m}{n+1} \tag{19}$$

Equation (19) is the probability of occurrence for each rank. The order given by *m* is also the order of harm caused by radioactive fallout [133].

This study also considered the harmonization of the important *pdf*s in the literature with the changes of ^{131}I in order to be able to make risk analyses and to find out the possibility of the occurrence of ^{131}I's activity in the research field and to find out the spatial transformations of these variables with the results obtained later. The calculations took into consideration three *pdf*s, which have the highest R^2.

Generalized extreme-value distribution

The generalized extreme-value distribution is based on the combination of Gumbel, Fréchet, and Weibull distributions and the continuous probability distributions developed within the extreme-value theory. The generalized extreme-value distribution can be used as an approach to model the maxima (or minima) of long (end) random sequences. As different from other distribution, it is represented by three parameters, namely, σ; scalar parameter, μ; location parameter and k; shape parameter.

The generalized extreme-value distribution is given by the following expression

$$f(x|k,\mu,\sigma) = \left(\frac{1}{\sigma}\right)\left(1 + k\frac{(x-\mu)}{\sigma}\right)^{-1-\frac{1}{k}} \exp\left(-\left(1 + k\frac{(x-\mu)}{\sigma}\right)^{-\frac{1}{k}}\right) \tag{20}$$

with $k \neq 0$ and $\left(1 + k\frac{(x-\mu)}{\sigma}\right) > 0$. The cumulative distribution function is then appears as follows.

$$F(x|k,\mu,\sigma) = \exp\left(-\left(1 + k\frac{(x-\mu)}{\sigma}\right)^{-\frac{1}{k}}\right) \tag{21}$$

with $k \neq 0$ and $\left(1 + k\frac{(x-\mu)}{\sigma}\right) > 0$.

The distribution has three alternatives according to the state of the *k* parameter: type 1 for $k = 0$, type 2 for $k > 0$ and type 3 for $k < 0$, which resemble Gumbel, Fréchet, and Weibull distributions, respectively [417–420]. The probability of non-occurrence for the generalized extreme-value distribution from Eq. (21) is given as,

$$g_{gev} = F(x \mid k, \ \mu, \ \sigma) \tag{22}$$

Again, from Eq. (14), the probability of occurrence becomes as,

$$r_{gev} = 1 - g_{gev} = 1 - F(x \mid k, \ \mu, \ \sigma) = 1 - \exp\left(-\left(1 + k\frac{(x-\mu)}{\sigma}\right)^{-\frac{1}{k}}\right) \tag{23}$$

Lognormal probability distribution

The lognormal distribution is a probability distribution for random variables, whose logarithm is normally distributed. If *x* shows lognormal distribution, then log(*x*) shows normal distribution. It does not matter what the basis for the logarithm function is. If $\log_a(x)$ shows the normal distribution for any two positive numbers *a*, $b \neq 1$, $\log_b(x)$ also implies normal distribution. Probability density function for lognormal distribution (μ; position parameter, σ; scale parameter and for $x > 0$) is

$$f(x \mid \mu, \ \sigma) = \left(\frac{1}{x \ln(\sigma)\sqrt{2\pi}}\right) \exp\left(-\frac{(\ln(x) - \ln(\mu))^2}{2\ln(\sigma)^2}\right) \tag{24}$$

The cumulative distribution function is given as

$$F(x \mid \mu, \ \sigma) = \frac{1}{\ln(\sigma)\sqrt{2\pi}} \int_0^x \frac{\exp\left(-\frac{(\ln(t)-\ln(\mu))^2}{2\ln(\sigma)^2}\right)}{t} dt \tag{25}$$

Lognormal *pdf* is a distribution function used to model randomly varying states [411].

Weibull probability distribution

The Weibull distribution is a probability distribution for random variables and its mathematical form is as follows.

$$f(x \mid \alpha, \ \beta) = \alpha\beta^{-\alpha}x^{\alpha-1} \exp\left(-\left(\frac{x}{\beta}\right)^{\alpha}\right) \tag{26}$$

where α is the shape parameter, and β is the scale parameter, and $x \geq 0$. The cumulative distribution function is then,

$$F(x \mid \alpha, \ \beta) = 1 - \exp\left(-\left(\frac{x}{\beta}\right)^{\alpha}\right) \tag{27}$$

[411].

Risk analysis and PDFs results

The activity values of the ^{131}I radioisotope, released after the Fukushima accident are not statistically discrete events; therefore, the probability curve for these activity values is the cumulative probability function. Equation (15) can be applied with the values in Table 4. For example, if the occurrence likelihood of activity value belonging to 10 stations is calculated, this probability value is equal to the sum of the occurrence likelihood of the activity value belonging to station 14 and the probability of occurrence between activity values of 2 stations. If this event is expressed with *A*, then from Eq. (15) the following expression is obtained.

$$P(A \leq 12610.98) = P(A \leq 11518.14) + P(11518.14 < A \leq 12610.98) \quad (28)$$

As can be understood from this equation, the probability functions are in cumulative form.

Sample risk calculations are given in Table 4, taking into account the 240th hour after the accident. In this table, the *g* probability of non-occurrence values are obtained from Eq. 17 and given in column 6, and the risk values from in Eq. 19 in column 7. The probabilities other hours are presented in Appendix C (supplementary material). The data are tested with important *pdf*s in the literature to see the probability of occurrence values for 19 stations. According to R^2 values, the most suitable *pdf*s are Weibull, Lognormal and Generalized Extreme-Value *pdf*s (Table 5), and *pdf*s with lower R^2 values from these three distributions are excluded from the calculations. The variables of the three distributions are calculated as in Table 6 with an illustration graph in Fig. 2 for the 240th hour. At all other times, the risk variance against radioactivity can be seen in Appendix D (supplementary material).

As for the R^2 values in Table 5, the generalized extreme-value distribution for all times is the most appropriate one. Another point to note is that the R^2 value of the generalized extreme-value distribution decreases with time.

Table 5 Correlation coefficients (R^2) of probability distribution functions

Time (h)	Weibull	Lognormal	Generalized extreme-value
240th	0.888712	0.940069	0.986169
360th	0.889536	0.940809	0.983607
480th	0.890289	0.941416	0.982529
600th	0.890981	0.941914	0.981845
720th	0.891347	0.941951	0.979861
840th	0.892154	0.942522	0.978637
960th	0.893021	0.943168	0.977732
1080th	0.894562	0.944512	0.977316
1200th	0.896613	0.946485	0.978036
1320th	0.898463	0.948219	0.978693
1440th	0.899907	0.949435	0.978789

Table 4 The probability of occurrence and probability of non-occurrence at 240th hour

Stations	Activity (Bq/kg)	Stations	Sorted activity (Bq/kg)	Rank (*m*)	Probability of nonoccurrence (*g*)	Probability of occurrence (*r*)
1	116,656.900	14	11,518.140	1	0.05	0.95
2	24,757.000	10	12,610.980	2	0.10	0.90
3	63,870.150	6	14,730.550	3	0.15	0.85
4	53,128.320	19	16,155.420	4	0.20	0.80
5	47,887.160	15	16,621.260	5	0.25	0.75
6	14,730.550	16	17,696.390	6	0.30	0.70
7	865,939.700	17	20,675.690	7	0.35	0.65
8	488,231.100	2	24,757.000	8	0.40	0.60
9	289,703.600	13	33,185.350	9	0.45	0.55
10	12,610.980	12	42,227.860	10	0.50	0.50
11	60,176.240	5	47,887.160	11	0.55	0.45
12	42,227.860	4	53,128.320	12	0.60	0.40
13	33,185.350	11	60,176.240	13	0.65	0.35
14	11,518.140	3	63,870.150	14	0.70	0.30
15	16,621.260	1	116,656.900	15	0.75	0.25
16	17,696.390	18	279,212.800	16	0.80	0.20
17	20,675.690	9	289,703.600	17	0.85	0.15
18	279,212.800	8	488,231.100	18	0.90	0.10
19	16,155.420	7	865,939.700	19	0.95	0.05

Table 6 Distribution functions of radioactivity with respect to the calculated hours and their parameters

Time (h)	Weibull		Lognormal		Generalized extreme-value		
	α	β	μ	σ	k	μ	σ
240th	0.723552	100,805.64	51,063.49	3.696306	1.552193	22,590.07	19,336.03
360th	0.720792	65,285.54	33,001.75	3.712866	1.565860	14,509.79	12,673.46
480th	0.717849	42,289.84	21,328.66	3.731421	1.501146	9576.53	8621.97
600th	0.714735	27,399.39	13,784.40	3.751977	1.413320	6385.04	5929.08
720th	0.711463	17,755.40	8908.748	3.774546	1.343775	4236.60	4043.69
840th	0.708046	11,508.10	5757.623	3.799133	1.290022	2797.48	2735.51
960th	0.704493	7460.350	3721.087	3.825752	1.247467	1840.53	1838.85
1080th	0.700818	4837.220	2404.896	3.854414	1.213026	1207.65	1230.01
1200th	0.697031	3136.990	1554.257	3.885124	1.184698	790.730	819.540
1320th	0.693143	2034.740	1004.499	3.917905	1.161139	516.890	544.310
1440th	0.689164	1320.020	649.1962	3.952764	1.141411	337.420	360.560

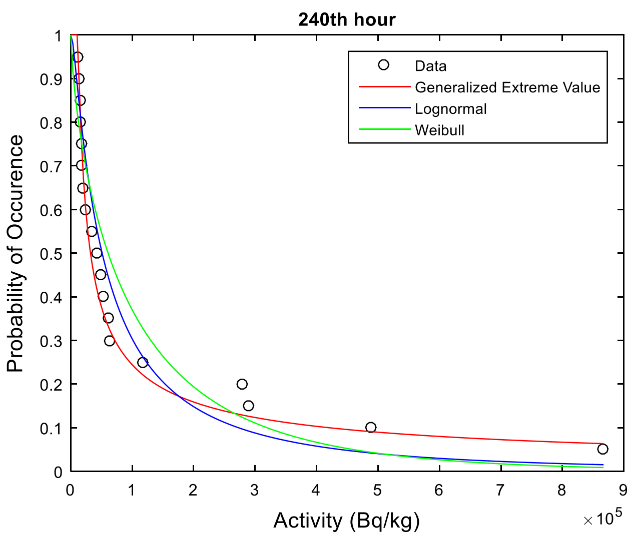

Fig. 2 The probability of occurrence (risk) graph against the 240th-hour activity

Furthermore, as time progresses, the risk caused by the fallout decreases.

A graph of the occurrence probability versus activity at 240th hour as an example is given in Fig. 2. One can see that the generalized extreme-value distribution explains the experimental data better than the other *pdf*s. For this reason, in the advanced risk analysis calculations, operations and interpretations are made by considering the generalized extreme value *pdf*. In Table 7, the risk, probability of occurrence and probability of non-occurrence values are calculated according to the generalized end-value distribution at the 240th hour and the station numbers are also given.

For instance, if the k, μ and σ parameters at 240th hour of generalized extreme-value distribution in Table 5 and the activity value (11,518.14 Bq/kg) at 14th station in Table 7 are substituted into Eq. (23), then r_{gev} is obtained from Eq. (29) (please refer to 4th column in Table 7). All the changes in other times are given in Appendix E (supplementary material).

$$r_{gud} = 1 - F(11518.14 \mid 1.552193,\ 22590.07,\ 19336.03)$$
$$r_{gev} = 1 - \exp\left(-\left(1 + 1.552193\frac{(11518.14 - 22590.07)}{19336.03}\right)^{-\frac{1}{1.552193}}\right)$$
$$r_{gev} = 0.983700 \tag{29}$$

Kriging methodology

The Kriging is an interpolation method developed by South African mining engineer Krige in the early 1960s and it is a local estimation technique in a region that provides the best linear objective estimate of the unknown characteristics. If one desires to make an estimate at point x_0 for $f(x)$ measurements taken against a value x in a region, it can be expressed as follows.

$$f(x_0) = \sum_{i=1}^{n} w_i(x_0) f(x_i) \tag{30}$$

In this equation, x_0 is the estimation point, $f(x_0)$ is the estimation value, and $w_i(x_0)$ are the weights, which are obtained from one of the covariance or variogram techniques [421]. The reason why Kriging differs from the classical linear regression is that the changes are not independent, and observations for the Kriging technique assume random sampling [422]. In this study, the Kriging method is used to obtain the surface maps of the ^{131}I radioactivity, probability of occurrence and non-occurrence of the activity.

Table 7 The probability of occurrence (risk) and probability of non-occurrence (confidence) according to the generalized extreme-value distribution at 240th hour

Stations	Activity (Bq/kg)	Probability of occurrence (risk) (r)	Generalized extreme-values, probability of occurrence (r_{gev})	Generalized extreme-values, probability of non-occurrence (g_{gev})
14	11,518.140	0.95	0.983700	0.016300
10	12,610.980	0.90	0.940996	0.059004
6	14,730.550	0.85	0.850516	0.149484
19	16,155.420	0.80	0.797531	0.202469
15	16,621.260	0.75	0.781794	0.218206
16	17,696.390	0.70	0.748203	0.251797
17	20,675.690	0.65	0.671588	0.328412
2	24,757.000	0.60	0.594177	0.405823
13	33,185.350	0.55	0.489650	0.510350
12	42,227.860	0.50	0.419290	0.580710
5	47,887.160	0.45	0.387075	0.612925
4	53,128.320	0.40	0.362491	0.637509
11	60,176.240	0.35	0.335184	0.664816
3	63,870.150	0.30	0.322901	0.677099
1	116,656.900	0.25	0.221919	0.778081
18	279,212.800	0.20	0.129011	0.870989
9	289,703.600	0.15	0.126078	0.873922
8	488,231.100	0.10	0.090970	0.909030
7	865,939.700	0.05	0.063444	0.936556

Kriging method results

The activity distribution map for ^{131}I after 240 h from the Fukushima accident using the Kriging method [423] is given in Fig. 3. The activity is in exponential decay with time, and hence, the simulation change is better observed at each hour.

In this study the half-circle area at sea is banned. Entrance and exit to this area are closed immediately after the accident. The data from MEXT correspond to the time when this region is forbidden (restricted). After the accident, only dose measurements are made with no activity measurements. The activity prediction maps obtained for all other prospective times are given in Appendix F (supplementary material). In addition, motion simulations of 60 days of activity change in ^{131}I are given in .mp4 format, Iodine131_Activity_Animated_Simulation_1.mp4 (Appendix G, supplementary material) file. When all of the maps in Fig. 3 and Appendix F (supplementary material) are examined, it is seen that ^{131}I activity values are high in the north-west and south part of Fukushima. In this case, it can be said that the ^{131}I core is moved north-west and southward after the accident. The map and animated simulations are available for 1440 h, or 60 days. Due to the short ^{131}I half-life, the activity value after 60 days has dropped to very low levels and experts have not been able to measure ^{131}I after the 60th day. As seen in the simulations, the activity values decrease rapidly with time progression.

The probability of occurrence according to the generalized extreme-value distribution, using activity values 240 h after the Fukushima accident is shown in Fig. 4 and the probability of absence in Fig. 5. The maps of these possibilities for all other times are given in Appendices H and I (supplementary material). The motion simulation files, in which the change of the event (activity concentration) and the absence of change after 60 days are estimated, are also given in .mp4 format in the form of Probability of Occurrence.mp4 (Appendix J, supplementary material) and Probability of Nonoccurrence.mp4 (Appendix K, supplementary material) files. These simulations allow seeing radioactive fallout as a whole for given hours.

Looking at Fig. 4 and all of the maps in Appendix H (supplementary material), the probability of occurrence value is close to 1 in the north and south-west part of Fukushima. In other words, it defines the probability of occurrence in regions with low activity and where repetition of these possibilities is the greatest. On the other hand, regions with high activity seem to protect these conditions. This is also radioactive emissions reporter from the reactor on a continuous basis during the period studied. In motion simulations that change the probability of occurrence (Probability of Occurrence.mp4, Appendix J, supplementary material), the areas where activity decreases as time elapses in the accident area can be seen clearly. These simulations allow one to see prospectively whether or not radioactivity is in an environment.

Fig. 3 ^{131}I radioactive fallout map at the 240th-hour

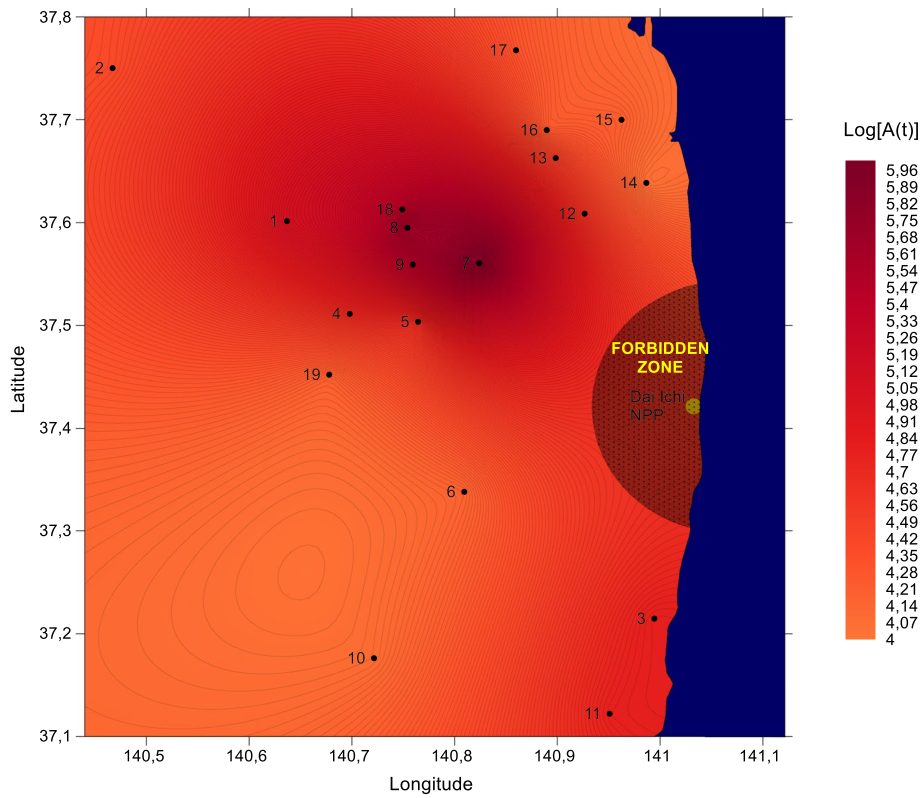

Fig. 4 Spatial variation of probability of occurrence (risk) according to the generalized extreme-value distribution corresponding to the activity values at 240th-hour

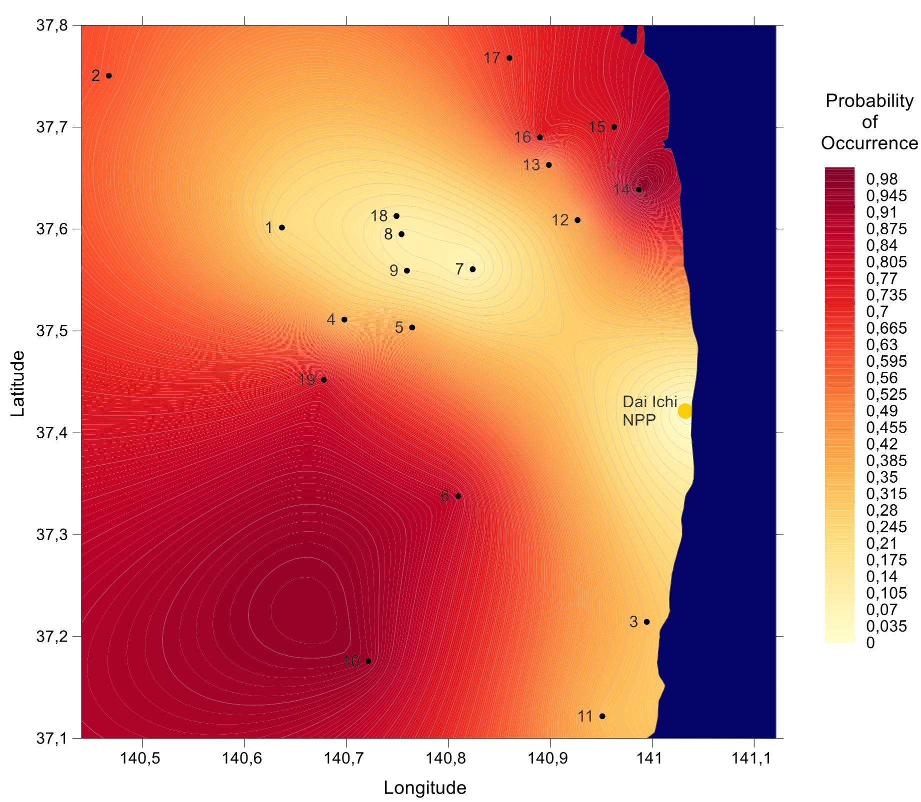

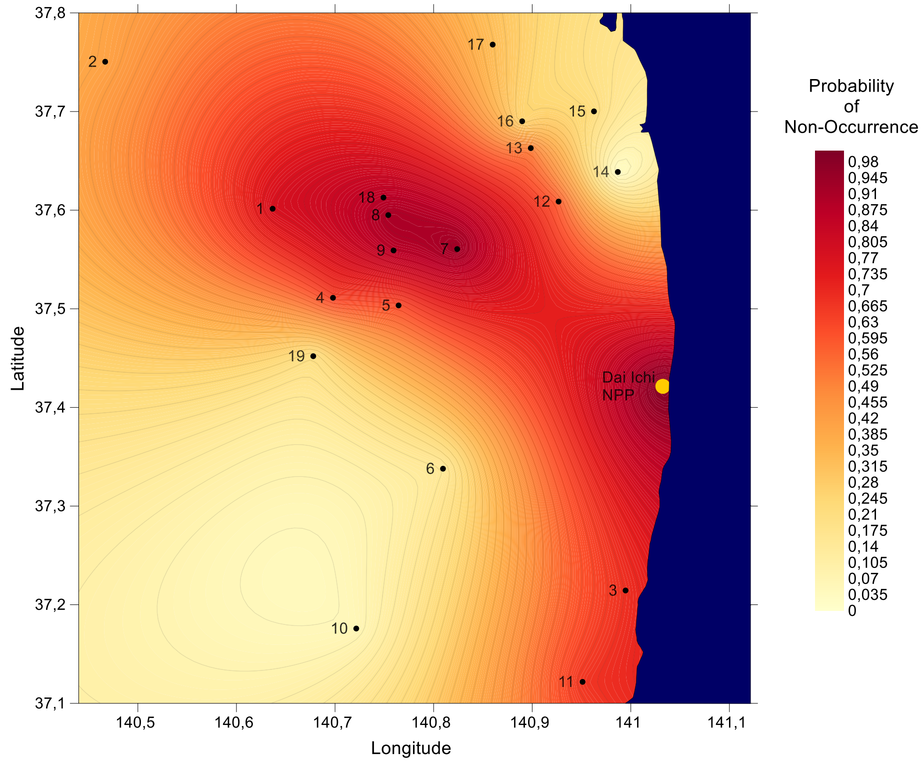

Fig. 5 Spatial variation of the probability of non-occurrence (confidence) values according to the generalized extreme-value distribution corresponding to the activity values at 240th-hour

Looking at the whole of the maps in Fig. 5 and Appendix I (supplementary material), the probability of non-occurrence of the activity in the north-eastern and south-western part of Fukushima is close to 0. This is in line with the assessment made for the activity maps. Since the activity values in these regions are close to 0, the probability of non-occurrence values approaches 0. The probability of non-occurrence decreases with time as it can be seen in moving simulation (Probability of Nonoccurrence.mp4, Appendix K, supplementary material).

Conclusions

Nuclear energy is one of the world's important energy sources, and its production is relatively cheap provided that the energy needs of nuclear power plants are supplied properly. Such a supply reduces the capital spent on energy production and increases purchasing power. This leads to an increase in the welfare level of any country, where nuclear energy investments exist. On the other hand, nuclear energy brings some risks in the event of a possible accident. However, it is possible to reduce the effects and risks that arise as a result of nuclear power plant accidents by employing scientific methodologies. Nonetheless, it can be said that nuclear energy is one of the sources with the lowest risk ratio in terms of both clean energy production and profit/loss balance, compared to other energy alternatives and the risks inherent in people's daily life. Through "Radioactive Waste Management", the possible risks that may arise are reduced to a minimum level. Nowadays, "Radioactive Waste Management" enables people to be affected radioactively at the minimum level through audits conducted by many organizations, especially by the International Atomic Energy Agency (IAEA). About 151 countries belonging to IAEA carry out Radioactive Waste Management, published by IAEA. At this point, countries are affected in their daily lives at a lower level of radiation. In addition, it is aimed to minimizing damage for the case of possible accidents. There are many studies for each stage of Radioactive Waste Management. Particularly after the Chernobyl accident, countries have begun to take strict measures, seeking answers to the questions "How should radioactive waste management done in the case of chaos?" Models have been proposed for radioisotope distributions in air, groundwater, sea, river, and soil. A realistic risk analysis model for radioactive fallout to be released after a possible accident will keep radioactive waste harms at the optimum level. On the other hand, this research also contributes considerably to Radioactive Waste Management and Radioactive Pollution Prevention Scenarios.

When FDNPPA was examined, it was observed that the results were generally non-linear, because radioactive materials that are emitted by atmospheres and other environmental systems are influenced in many ways from atmospheric pressure to the humidity of the environment. Artificial intelligence techniques such as artificial neural networks and fuzzy logic can be used in future models for similar studies. In other respects, chaotic calculations provide effective results for non-linear studies and they can be applied as other different steps for this and similar studies. After FDNPPA, the activity of the short half-life ^{131}I isotope was taken at 19 different stations at different times. The fact that activity measurements are not synchronous in a research area is the main reason why the distribution of radioactivity in that area cannot be determined as a whole. If this research is to be carried out with a long half-life radioisotope, such as ^{134}Cs or ^{137}Cs, the daily, weekly or even monthly change in activity would be almost constant or would show a linear change. In this case, a single scattering graph coupled with risk assessment is sufficient for long-life radioisotopes. The change in activity values for the short half-life of ^{131}I (approx. 8 days) is shorter, but at some stations (stations 3, 6, 7, 16, and 19), measurements take long intervals, as simultaneous measurements are not taken from the stations. In this case, model curves are recommended to each station for accurate results in a risk assessment at a given time. The studied parameter is activity and the variation is visibly exponential, and hence, this model is obtained by the least squares method. In this study, a risk analysis method is developed to determine the risk levels of non-asynchronous radioactivity data. The power of Least Squares Method in obtaining simultaneous data is percieved. After getting the risk values of the simultaneous data, it is decided that the *pdf*, which best describes these risk values, is the Generalized Extreme-Value Distribution (GEVD). In the literature, GEVD is a type of distribution proposed for the data under a sudden development of chaotic conditions. The activity a value of the ^{131}I radioisotope is released after the FDNPP accident, which is a chaotic situation, and they are expected to comply with GEVD. As the time progresses, the activity values of the stations change, but the suitability of GEVD remains unchanged. Hence, the activity risk values in the GEVD are equivalent to saying that the GEVD is a characteristic of the activities in this region. It is then expected that as the value of activity decreases, the appropriateness of the GEVD decreases. As a result, for Fukushima, it can be said, "the risk distribution according to the position of ^{131}I corresponds to the GEVD".

Changes in the ^{131}I contamination probability to occur and not to arrive are determined for the next 60 days after the accident. These possibilities are shown on maps and as simulation animations, which prospectively made it possible to glimpse the possibility of radioactivity being in an environment or not. The simulation method gives instant information for the risk levels that the corresponding radionuclide generates leading to a strong belief that it can be easily used in other similar studies.

With the methodologies proposed in this study, if the examined radionuclide has a long half-life, it can display moving or still simulation images; sampling areas can be expanded to reach global measurements in terms of both distance and duration. Especially, moving simulations help to facilitate the interpretation of the case/event of the scientists, who can work on the advanced subject. With this simulation method, it is possible to observe the spread of radioactivity over ground layers, as well as the propagation of atmospheric radioactive fallout.

Acknowledgements This research was supported by Firat University (Grant Number: FF.12.25). We are grateful to the Editor-in-Chief (Prof Zsolt Revay) and two anonymous referees for their outstanding support in the investigation and development of this research.

References

1. Book reviews (1975) Ann Assoc Am Geogr 65(2):313–337. https://doi.org/10.1111/j.1467-8306.1975.tb01039.x
2. Krivit S, Lehr J, Kingery T (2011) Nuclear energy encyclopedia—science, technology and applications. Wiley series on energy. Wiley, New York
3. WHO reports low health risk from Fukushima (2013) Nucl Eng Int 58 (705):26–29
4. Akai J, Anawar HM (2013) Mineralogical approach in elucidation of contamination mechanism for toxic trace elements in the environment: special reference to arsenic contamination in groundwater. Phys Chem Earth 58–60:2–12. https://doi.org/10.1016/j.pce.2013.04.011
5. Changlai SP, Tsai HH, Tsai SC, Chen HP, Chang CL, Yao YH, Chen CY (2012) Environmental radiation detected at Lin Shin Hospital in Taichung during the Fukushima nuclear power plant accident. J Radioanal Nucl Chem 291(3):859–863. https://doi.org/10.1007/s10967-011-1376-4
6. Ioannides K, Stamoulis K, Papachristodoulou C (2013) Environmental radioactivity measurements in north-western Greece following the Fukushima nuclear accident. J Radioanal Nucl Chem 298(2):1207–1213. https://doi.org/10.1007/s10967-013-2527-6
7. Manolopoulou M, Stoulos S, Ioannidou A, Vagena E, Papastefanou C (2012) Radiation measurements and radioecological aspects of fallout from the Fukushima nuclear accident. J Radioanal Nucl Chem 292(1):155–159. https://doi.org/10.1007/s10967-011-1386-2
8. Bortz F (2012) Meltdown! The nuclear disaster in Japan and our energy future. Twenty-First Century Books, Lerner, ISBN: 978-0-7613-8660-5
9. Sinclair L, Seywerd H, Fortin R, Carson J, Saull P, Coyle M, Van Brabant R, Buckle J, Desjardins S, Hall R (2011) Aerial measurement of radioxenon concentration off the west coast of Vancouver Island following the Fukushima reactor accident. J Environ Radioact 102(11):1018–1023
10. Unno N, Minakami H, Kubo T, Fujimori K, Ishiwata I, Terada H, Saito S, Yamaguchi I, Kunugita N, Nakai A, Yoshimura Y (2012) Effect of the Fukushima nuclear power plant accident on radioiodine (131I) content in human breast milk. J Obstet Gynaecol Res 38(5):772–779. https://doi.org/10.1111/j.1447-0756.2011.01810.x
11. Xu S, Cook GT, Cresswell AJ, Dunbar E, Freeman S, Hastie H, Hou XL, Jacobsson P, Naysmith P, Sanderson DCW, Tripney BG, Yamaguchi K (2016) C-14 levels in the vicinity of the Fukushima Dai-ichi nuclear power plant prior to the 2011 accident. J Environ Radioact 157:90–96. https://doi.org/10.1016/j.jenvrad.2016.03.013

12. Xu S, Freeman S, Hou XL, Watanabe A, Yamaguchi K, Zhang LY (2013) Iodine isotopes in precipitation: temporal responses to I-129 emissions from the Fukushima nuclear accident. Environ Sci Technol 47(19):10851–10859. https://doi.org/10.1021/es401527q
13. Xu S, Zhang LY, Freeman S, Hou XL, Yamaguchi K, Cresswell AJ, Sanderson DCW (2016) I-129 and Cs-137 in groundwater in the vicinity of Fukushima Dai-ichi nuclear power plant. Geochem J 50(3):287–291. https://doi.org/10.2343/geochemj.2.0414
14. Yamaguchi N, Eguchi S, Fujiwara H, Hayashi K, Tsukada H (2012) Radiocesium and radioiodine in soil particles agitated by agricultural practices: field observation after the Fukushima nuclear accident. Sci Total Environ 425:128–134. https://doi.org/10.1016/j.scitotenv.2012.02.037
15. Yamaguchi T, Sawano K, Kishimoto M, Furuhama K, Yamada K (2012) Early-stage bioassay for monitoring radioactive contamination in living livestock. J Vet Med Sci 74(12):1675–1676. https://doi.org/10.1292/jvms.12-0170
16. Momoshima N, Sugihara S, Ichikawa R, Yokoyama H (2012) Atmospheric radionuclides transported to Fukuoka, Japan remote from the Fukushima Dai-ichi nuclear power complex following the nuclear accident. J Environ Radioact 111:28–32. https://doi.org/10.1016/j.jenvrad.2011.09.001
17. Bolsunovsky A, Dementyev D (2011) Evidence of the radioactive fallout in the center of Asia (Russia) following the Fukushima nuclear accident. J Environ Radioact 102(11):1062–1064
18. Tagami K, Uchida S (2011) Can we remove iodine-131 from tap water in Japan by boiling? Experimental testing in response to the Fukushima Daiichi nuclear power plant accident. Chemosphere 84(9):1282–1284. https://doi.org/10.1016/j.chemosphere.2011.05.050
19. Tagami K, Uchida S, Uchihori Y, Ishii N, Kitamura H, Shirakawa Y (2011) Specific activity and activity ratios of radionuclides in soil collected about 20 km from the Fukushima Daiichi nuclear power plant: radionuclide release to the south and southwest. Sci Total Environ 409(22):4885–4888. https://doi.org/10.1016/j.scitotenv.2011.07.067
20. Morino Y, Ohara T, Nishizawa M (2011) Atmospheric behavior, deposition, and budget of radioactive materials from the Fukushima Daiichi nuclear power plant in March 2011. Geophys Res Lett. https://doi.org/10.1029/2011gl048689
21. Huh C-A, Hsu S-C, Lin C-Y (2012) Fukushima-derived fission nuclides monitored around Taiwan: free tropospheric versus boundary layer transport. Earth Planet Sci Lett 319:9–14
22. Manolopoulou M, Vagena E, Stoulos S, Ioannidou A, Papastefanou C (2011) Radioiodine and radiocesium in Thessaloniki, Northern Greece due to the Fukushima nuclear accident. J Environ Radioact 102(8):796–797. https://doi.org/10.1016/j.jenvrad.2011.04.010
23. Masson O, Baeza A, Bieringer J, Brudecki K, Bucci S, Cappai M, Carvalho FP, Connan O, Cosma C, Dalheimer A, Didier D, Depuydt G, De Geer LE, De Vismes A, Gini L, Groppi F, Gudnason K, Gurriaran R, Hainz D, Halldorsson O, Hammond D, Hanley O, Holey K, Homoki Z, Ioannidou A, Isajenko K, Jankovic M, Katzlberger C, Kettunen M, Kierepko R, Kontro R, Kwakman PJM, Lecomte M, Vintro LL, Leppanen AP, Lind B, Lujaniene G, Mc Ginnity P, Mc Mahon C, Mala H, Manenti S, Manolopoulou M, Mattila A, Mauring A, Mietelski JW, Moller B, Nielsen SP, Nikolic J, Overwater RMW, Palsson SE, Papastefanou C, Penev I, Pham MK, Povinec PP, Rameback H, Reis MC, Ringer W, Rodriguez A, Rulik P, Saey PRJ, Samsonov V, Schlosser C, Sgorbati G, Silobritiene BV, Soderstrom C, Sogni R, Solier L, Sonck M, Steinhauser G, Steinkopff T, Steinmann P, Stoulos S, Sykora I, Todorovic D, Tooloutalaie N, Tositti L, Tschiersch J, Ugron A, Vagena E, Vargas A, Wershofen H, Zhukova O (2011) Tracking of airborne radionuclides from the damaged Fukushima Dai-Ichi nuclear reactors by European networks. Environ Sci Technol 45(18):7670–7677. https://doi.org/10.1021/es2017158
24. Lozano R, Hernández-Ceballos M, Adame J, Casas-Ruíz M, Sorribas M, San Miguel E, Bolívar J (2011) Radioactive impact of Fukushima accident on the Iberian Peninsula: evolution and plume previous pathway. Environ Int 37(7):1259–1264
25. Pittauerová D, Hettwig B, Fischer HW (2011) Fukushima fallout in Northwest German environmental media. J Environ Radioact 102(9):877–880
26. Katata G, Chino M, Kobayashi T, Terada H, Ota M, Nagai H, Kajino M, Draxler R, Hort M, Malo A (2015) Detailed source term estimation of the atmospheric release for the Fukushima Daiichi Nuclear Power Station accident by coupling simulations of an atmospheric dispersion model with an improved deposition scheme and oceanic dispersion model. Atmos Chem Phys 15(2):1029–1070
27. Yoshida N, Kanda J (2012) Tracking the Fukushima radionuclides. Science 336(6085):1115–1116
28. Minowa H (2015) Image analysis of radiocesium distribution in coniferous trees two years after the Fukushima Daiichi nuclear power plant accident. J Radioanal Nucl Chem 303(2):1601–1605. https://doi.org/10.1007/s10967-014-3817-3
29. Aliyu AS, Evangeliou N, Mousseau TA, Wu J, Ramli AT (2015) An overview of current knowledge concerning the health and environmental consequences of the Fukushima Daiichi nuclear power plant (FDNPP) accident. Environ Int 85:213–228
30. Kuramochi T (2015) Review of energy and climate policy developments in Japan before and after Fukushima. Renew Sustain Energy Rev 43:1320–1332. https://doi.org/10.1016/j.rser.2014.12.001
31. Poumadere M, Bertoldo R, Samadi J (2011) Public perceptions and governance of controversial technologies to tackle climate change: nuclear power, carbon capture and storage, wind, and geoengineering. Wiley Interdiscip Rev Clim Change 2(5):712–727. https://doi.org/10.1002/wcc.134
32. Jones CR, Elgueta H, Eiser JR (2016) Reconciling nuclear risk: the impact of the Fukushima accident on comparative preferences for nuclear power in UK electricity generation. J Appl Soc Psychol 46(4):242–256. https://doi.org/10.1111/jasp.12359
33. Karakosta C, Pappas C, Marinakis V, Psarras J (2013) Renewable energy and nuclear power towards sustainable development: characteristics and prospects. Renew Sust Energy Rev 22:187–197. https://doi.org/10.1016/j.rser.2013.01.035
34. Kuramochi T, Wakiyama T, Kuriyama A (2017) Assessment of national greenhouse gas mitigation targets for 2030 through meta-analysis of bottom-up energy and emission scenarios: a case of Japan. Renew Sustain Energy Rev 77:924–944. https://doi.org/10.1016/j.rser.2016.12.093
35. Kusumi T, Hirayama R, Kashima Y (2017) Risk perception and risk talk: the case of the Fukushima Daiichi nuclear radiation risk. Risk Anal 37(12):2305–2320. https://doi.org/10.1111/risa.12784
36. Pravalie R, Bandoc G (2018) Nuclear energy: between global electricity demand, worldwide decarbonisation imperativeness, and planetary environmental implications. J Environ Manage 209:81–92. https://doi.org/10.1016/j.jenvman.2017.12.043
37. Wang GA, Li JR, Ravi S, Van Pelt RS, Costa PJM, Dukes D (2017) Tracer techniques in aeolian research: approaches, applications, and challenges. Earth Sci Rev 170:1–16. https://doi.org/10.1016/j.earscirev.2017.05.001
38. Klein SA, Hall A, Norris JR, Pincus R (2017) Low-cloud feedbacks from cloud-controlling factors: a review. Surv Geophys 38(6):1307–1329. https://doi.org/10.1007/s10712-017-9433-3
39. Slangen ABA, Adloff F, Jevrejeva S, Leclercq PW, Marzeion B, Wada Y, Winkelmann R (2017) A review of recent updates of

sea-level projections at global and regional scales. Surv Geophys 38(1):385–406. https://doi.org/10.1007/s10712-016-9374-2
40. Vial J, Bony S, Stevens B, Vogel R (2017) Mechanisms and model diversity of trade-wind shallow cumulus cloud feedbacks: a review. Surv Geophys 38(6):1331–1353. https://doi.org/10.1007/s10712-017-9418-2
41. Wing AA, Emanuel K, Holloway CE, Muller C (2017) Convective self-aggregation in numerical simulations: a review. Surv Geophys 38(6):1173–1197. https://doi.org/10.1007/s10712-017-9408-4
42. Hirose K (2018) Long-term monitoring of radiocesium deposition near the Fukushima Dai-ichi nuclear power plant: effect of interception of radiocesium on vegetables. J Radioanal Nucl Chem 318(1):65–70. https://doi.org/10.1007/s10967-018-5972-4
43. Fujimura S, Ishikawa J, Sakuma Y, Saito T, Sato M, Yoshioka K (2014) Theoretical model of the effect of potassium on the uptake of radiocesium by rice. J Environ Radioact 138:122–131. https://doi.org/10.1016/j.jenvrad.2014.08.017
44. Hermsmeyer S, Herranz LE, Iglesias R, Reer B, Nowack H, Sonnenkalb M, Stefanova A, Chatelard P, Foucher L, Raimond E, Barnak M, Matejovic P, Sanchez V, Lajtha G, Techy Z, Lind T, Gremme F, Koch M, Bujan A, Grah A, Pascal G, Pla P, Sangiorgi M, Strucic M, Garcia MV (2015) Review of current severe accident management approaches in Europe and identification of related modelling requirements for the computer code ASTEC V2.1. Atw-Int J Nucl Power 60(7):461–+
45. Ryu Y, Kim S (2015) Testing the heuristic/systematic information-processing model (HSM) on the perception of risk after the Fukushima nuclear accidents. J Risk Res 18(7):840–859. https://doi.org/10.1080/13669877.2014.910694
46. Sutou S (2015) Tremendous human, human, social, and economic losses caused by obstinate application of the failed linear no-threshold model. Yakugaku Zasshi-J Pharm Soc Jpn 135(11):1197–1211. https://doi.org/10.1248/yakushi.15-00188
47. Srinivas CV, Rakesh PT, Prasad K, Venkatesan R, Baskaran R, Venkatraman B (2014) Assessment of atmospheric dispersion and radiological impact from the Fukushima accident in a 40-km range using a simulation approach. Air Qual Atmos Health 7(2):209–227. https://doi.org/10.1007/s11869-014-0241-3
48. Hidaka A, Yokoyama H (2017) Examination of I-131 and Cs-137 releases during late phase of Fukushima Daiichi NPP accident by using I-131/Cs-137 ratio of source terms evaluated reversely by WSPEEDI code with environmental monitoring data. J Nucl Sci Technol 54(8):819–829. https://doi.org/10.1080/00223131.2017.1323691
49. Kaeriyama H (2017) Oceanic dispersion of Fukushima-derived radioactive cesium: a review. Fish Oceanogr 26(2):99–113. https://doi.org/10.1111/fog.12177
50. Aliyu AS, Evangeliou N, Mousseau TA, Wu JW, Ramli AT (2015) An overview of current knowledge concerning the health and environmental consequences of the Fukushima Daiichi nuclear power plant (FDNPP) accident. Environ Int 85:213–228. https://doi.org/10.1016/j.envint.2015.09.020
51. Bottomley PDW, Walker CT, Papaioannou D, Bremier S, Poml P, Glatz JP, van Winckel S, van Uffelen P, Manara D, Rondinella VV (2014) Severe accident research at the Transuranium Institute Karlsruhe: a review of past experience and its application to future challenges. Ann Nucl Energy 65:345–356. https://doi.org/10.1016/j.anucene.2013.11.012
52. Bridgman S (2001) Community health risk assessment after a fire with asbestos containing fallout. J Epidemiol Community Health 55(12):921–927. https://doi.org/10.1136/jech.55.12.921
53. Cho HS, Woo TH (2017) Real-time management (RTM) by cloud computing system dynamics (CCSD) for risk analysis of Fukushima nuclear power plant (NPP) accident. Atw-Int J Nucl Power 62 (3):171–+
54. Evrard O, Laceby JP, Lepage H, Onda Y, Cerdan O, Ayrault S (2015) Radiocesium transfer from hillslopes to the Pacific Ocean after the Fukushima nuclear power plant accident: a review. J Environ Radioact 148:92–110. https://doi.org/10.1016/j.jenvrad.2015.06.018
55. Gusman AR, Satake K, Shinohara M, Sakai S, Tanioka Y (2017) Fault Slip Distribution of the 2016 Fukushima Earthquake Estimated from Tsunami Waveforms. Pure appl Geophys 174(8):2925–2943. https://doi.org/10.1007/s00024-017-1590-2
56. Hirose K (2016) Fukushima Daiichi nuclear plant accident: atmospheric and oceanic impacts over the five years. J Environ Radioact 157:113–130. https://doi.org/10.1016/j.jenvrad.2016.01.011
57. Huang L, Zhou Y, Han YT, Hammitt JK, Bi J, Liu Y (2013) Effect of the Fukushima nuclear accident on the risk perception of residents near a nuclear power plant in China. Proc Natl Acad Sci USA 110(49):19742–19747. https://doi.org/10.1073/pnas.1313825110
58. Huh CA, Lin CY, Hsu SC (2013) Regional dispersal of Fukushima-derived fission nuclides by East-Asian monsoon: a synthesis and review. Aerosol Air Qual Res 13(2):537–544. https://doi.org/10.4209/aaqr.2012.08.0223
59. Iimura A, Cross JS (2016) Influence of safety risk perception on post-Fukushima generation mix and its policy implications in Japan. Asia Pac Policy Stud 3(3):518–532. https://doi.org/10.1002/app5.151
60. Kakamu T, Hidaka T, Hayakawa T, Kumagai T, Jinnouchi T, Tsuji M, Nakano S, Koyama K, Fukushima T (2015) Risk and preventive factors for heat illness in radiation decontamination workers after the Fukushima Daiichi nuclear power plant accident. J Occup Health 57(4):331–338. https://doi.org/10.1539/joh.14-0218-OA
61. Kamae K (2016) Earthquakes, tsunamis and nuclear risks: prediction and assessment beyond the Fukushima accident. Springer, Tokyo. https://doi.org/10.1007/978-4-431-55822-4
62. Kimura AH (2017) Fukushima ETHOS: post-disaster risk communication, affect, and shifting risks. Sci Cult. https://doi.org/10.1080/09505431.2017.1325458
63. Lei H, Yuting H, Jun B, Ying Z, Yang L, Hammitt JK (2013) Effect of the Fukushima nuclear accident on the risk perception of residents near a nuclear power plant in China. Proc Natl Acad Sci USA 110(49):19742–19747. https://doi.org/10.1073/pnas.1313825110
64. Makowski P, Deschanels X, Grandjean A, Meyer D, Toquer G, Goettmann F (2012) Mesoporous materials in the field of nuclear industry: applications and perspectives. New J Chem 36(3):531–541. https://doi.org/10.1039/c1nj20703b
65. Nishimura T, Hoshi H, Hotta A (2015) Current research and development activities on fission products and hydrogen risk after the accident at Fukushima Daiichi nuclear power station. Nucl Eng Technol 47(1):1–10. https://doi.org/10.1016/j.net.2014.12.002
66. Prati G, Zani B (2013) The effect of the Fukushima nuclear accident on risk perception, antinuclear behavioral intentions, attitude, trust, environmental beliefs, and values. Environ Behav 45(6):782–798. https://doi.org/10.1177/0013916512444286
67. Riedlinger M, Rea J (2015) Discourse ecology and knowledge niches: negotiating the risks of radiation in online Canadian forums, Post-Fukushima. Sci Technol Hum Values 40(4):588–614. https://doi.org/10.1177/0162243915571166
68. Zheng J, Tagami K, Uchida S (2013) Release of plutonium isotopes into the environment from the Fukushima Daiichi nuclear power plant accident: what is known and what needs to be known. Environ Sci Technol 47(17):9584–9595. https://doi.org/10.1021/es402212v

69. Tanaka S, Zabel J (2018) Valuing nuclear energy risk: evidence from the impact of the Fukushima crisis on U.S. house prices. J Environ Econ Manag 88:411–426. https://doi.org/10.1016/j.jeem.2017.12.005
70. Takebayashi Y, Lyamzina Y, Suzuki Y, Murakami M (2017) Risk perception and anxiety regarding radiation after the 2011 Fukushima nuclear power plant accident: a systematic qualitative review. Int J Env Res Public Health 14(11):1306. https://doi.org/10.3390/ijerph14111306
71. Kristiansen NI, Stohl A, Wotawa G (2012) Atmospheric removal times of the aerosol-bound radionuclides 137 Cs and 131 I measured after the Fukushima Dai-ichi nuclear accident–a constraint for air quality and climate models. Atmos Chem Phys 12(22):10759–10769
72. Aoyama M (2014) Transport processes of Fukushima derived radioactivity in the Pacific Ocean. Yakugaku Zasshi-J Pharm Soc Jpn 134(2):149–154. https://doi.org/10.1248/yakushi.13-00227-3
73. Ashraf MA, Khan AM, Ahmad M, Akib S, Balkhair KS, Abu Bakar NK (2014) Release, deposition and elimination of radiocesium (Cs-137) in the terrestrial environment. Environ Geochem Health 36(6):1165–1190. https://doi.org/10.1007/s10653-014-9620-9 **(Retracted article. See vol. 39, pg. 703, 2017)**
74. Buesseler K, Dai MH, Aoyama M, Benitez-Nelson C, Charmasson S, Higley K, Maderich V, Masque P, Morris PJ, Oughton D, Smith JN, Annual R (2017) Fukushima Daiichi-derived radionuclides in the ocean: transport, fate, and impacts. In: Annual review of marine sciences, vol 9, pp 173–203. https://doi.org/10.1146/annurev-marine-010816-060733
75. Kumamoto Y, Aoyama M, Hamajima Y, Nagai H, Yamagata T, Murata A (2017) Spreading of Fukushima-derived radiocesium in the Western North Pacific Ocean by the end of 2014. Bunseki Kagaku 66(3):137–148. https://doi.org/10.2116/bunsekikagaku.66.137
76. Nollet KE, Ohto H, Yasuda H, Hasegawa A (2013) The Great East Japan Earthquake of March 11, 2011, from the vantage point of blood banking and transfusion medicine. Transfus Med Rev 27(1):29–35. https://doi.org/10.1016/j.tmrv.2012.07.001
77. Prants SV (2014) Chaotic Lagrangian transport and mixing in the ocean. Eur Phys J-Spec Top 223(13):2723–2743. https://doi.org/10.1140/epjst/e2014-02288-5
78. Wang XY, Kato H, Shibasaki R (2013) Risk perception and communication in international maritime shipping in Japan after the Fukushima Daiichi nuclear power plant disaster. Transp Res Rec 2330:87–94. https://doi.org/10.3141/2330-12
79. Harrison RG (2004) The global atmospheric electrical circuit and climate. Surv Geophys 25(5–6):441–484. https://doi.org/10.1007/s10712-004-5439-8
80. Mathieu A, Korsakissok I, Quélo D, Saunier O, Groëll J, Didier D, Corbin D, Denis J, Tombette M, Winiarek V, Bocquet M, Quentric E, Benoit JP (2013) State of the model to simulate the Fukushima Daiichi nuclear power plant accident. Pollut Atmos. https://doi.org/10.4267/pollution-atmospherique.955
81. Saunier O, Mathieu A, Didier D, Tombette M, Quelo D, Winiarek V, Bocquet M (2013) An inverse modeling method to assess the source term of the Fukushima nuclear power plant accident using gamma dose rate observations. Atmos Chem Phys 13(22):11403–11421. https://doi.org/10.5194/acp-13-11403-2013
82. Winiarek V, Bocquet M, Duhanyan N, Roustan Y, Saunier O, Mathieu A (2014) Estimation of the caesium-137 source term from the Fukushima Daiichi nuclear power plant using a consistent joint assimilation of air concentration and deposition observations. Atmos Environ 82:268–279. https://doi.org/10.1016/j.atmosenv.2013.10.017
83. Christoudias T, Lelieveld J (2013) Modelling the global atmospheric transport and deposition of radionuclides from the Fukushima Dai-ichi nuclear accident. Atmos Chem Phys 13(3):1425–1438. https://doi.org/10.5194/acp-13-1425-2013
84. Geng X, Xie Z, Zhang L, Xu M, Jia B (2018) An inverse method to estimate emission rates based on nonlinear least-squares-based ensemble four-dimensional variational data assimilation with local air concentration measurements. J Environ Radioact 183:17–26. https://doi.org/10.1016/j.jenvrad.2017.12.004
85. Kadowaki M, Nagai H, Terada H, Katata G, Akari S (2017) Improvement of atmospheric dispersion simulation using an advanced meteorological data assimilation method to reconstruct the spatiotemporal distribution of radioactive materials released during the Fukushima Daiichi Nuclear Power Station accident. In: Kobayashi Y, Chiba S, Obara T et al (eds) Special Issue of for the fifth international symposium on innovative nuclear energy systems, vol 131. Energy Procedia. Elsevier Science Bv, Amsterdam, pp 208–215. https://doi.org/10.1016/j.egypro.2017.09.465
86. Katata G, Chino M, Kobayashi T, Terada H, Ota M, Nagai H, Kajino M, Draxler R, Hort MC, Malo A, Torii T, Sanada Y (2015) Detailed source term estimation of the atmospheric release for the Fukushima Daiichi Nuclear Power Station accident by coupling simulations of an atmospheric dispersion model with an improved deposition scheme and oceanic dispersion model. Atmos Chem Phys 15(2):1029–1070. https://doi.org/10.5194/acp-15-1029-2015
87. Hirao S, Yamazawa H, Nagae T (2013) Estimation of release rate of iodine-131 and cesium-137 from the Fukushima Daiichi nuclear power plant: Fukushima NPP accident related. J Nucl Sci Technol 50(2):139–147
88. Chino M, Nakayama H, Nagai H, Terada H, Katata G, Yamazawa H (2011) Preliminary estimation of release amounts of 131I and 137Cs accidentally discharged from the Fukushima Daiichi nuclear power plant into the atmosphere. J Nucl Sci Technol 48(7):1129–1134
89. Korsakissok I, Mathieu A, Didier D (2013) Atmospheric dispersion and ground deposition induced by the Fukushima nuclear power plant accident: a local-scale simulation and sensitivity study. Atmos Environ 70:267–279. https://doi.org/10.1016/j.atmosenv.2013.01.002
90. Kristiansen NI, Stohl A, Wotawa G (2012) Atmospheric removal times of the aerosol-bound radionuclides Cs-137 and I-131 measured after the Fukushima Dai-ichi nuclear accident—a constraint for air quality and climate models. Atmos Chem Phys 12(22):10759–10769. https://doi.org/10.5194/acp-12-10759-2012
91. Saunier O, Mathieu A, Didier D, Tombette M, Quélo D, Winiarek V, Bocquet M (2013) An inverse modeling method to assess the source term of the Fukushima nuclear power plant accident using gamma dose rate observations. Atmos Chem Phys 13(22):11403–11421. https://doi.org/10.5194/acp-13-11403-2013
92. Stohl A, Seibert P, Wotawa G, Arnold D, Burkhart JF, Eckhardt S, Tapia C, Vargas A, Yasunari TJ (2012) Xenon-133 and caesium-137 releases into the atmosphere from the Fukushima Dai-ichi nuclear power plant: determination of the source term, atmospheric dispersion, and deposition. Atmos Chem Phys 12(5):2313–2343. https://doi.org/10.5194/acp-12-2313-2012
93. Yasunari TJ, Stohl A, Hayano RS, Burkhart JF, Eckhardt S, Yasunari T (2011) Cesium-137 deposition and contamination of Japanese soils due to the Fukushima nuclear accident. Proc Natl Acad Sci USA 108(49):19530–19534. https://doi.org/10.1073/pnas.1112058108
94. Winiarek V, Bocquet M, Saunier O, Mathieu A (2012) Estimation of errors in the inverse modeling of accidental release of atmospheric pollutant: Application to the reconstruction of the cesium-137 and iodine-131 source terms from the Fukushima Daiichi power plant. J Geophys Res Atmos. https://doi.org/10.1029/2012jd018107

95. Kosaka K, Asami M, Kobashigawa N, Ohkubo K, Terada H, Kishida N, Akiba M (2012) Removal of radioactive iodine and cesium in water purification processes after an explosion at a nuclear power plant due to the Great East Japan Earthquake. Water Res 46(14):4397–4404
96. Miyazaki H, Tsuchiyama T, Terada H (2013) Examination of radioactive contamination in foods. Food Hyg Saf Sci 54(2):156–164. https://doi.org/10.3358/shokueishi.54.156
97. Terada H, Katata G, Chino M, Nagai H (2012) Atmospheric discharge and dispersion of radionuclides during the Fukushima Dai-ichi nuclear power plant accident. Part II: verification of the source term and analysis of regional-scale atmospheric dispersion. J Environ Radioact 112:141–154. https://doi.org/10.1016/j.jenvrad.2012.05.023
98. Masson O, Ringer W, Malá H, Rulik P, Dlugosz-Lisiecka M, Eleftheriadis K, Meisenberg O, De Vismes-Ott A, Fo Gensdarmes (2013) Size distributions of airborne radionuclides from the Fukushima nuclear accident at several places in Europe. Environ Sci Technol 47(19):10995–11003
99. Long NQ, Truong Y, Hien PD, Binh NT, Sieu L, Giap T, Phan N (2012) Atmospheric radionuclides from the Fukushima Dai-ichi nuclear reactor accident observed in Vietnam. J Environ Radioact 111:53–58
100. Kim C-K, Byun J-I, Chae J-S, Choi H-Y, Choi S-W, Kim D-J, Kim Y-J, Lee D-M, Park W-J, Yim SA (2012) Radiological impact in Korea following the Fukushima nuclear accident. J Environ Radioact 111:70–82
101. Xu S, Freeman SP, Hou X, Watanabe A, Yamaguchi K, Zhang L (2013) Iodine isotopes in precipitation: temporal responses to 129I emissions from the Fukushima nuclear accident. Environ Sci Technol 47(19):10851–10859
102. Arai T (2016) Temporal and spatial variations of radioactive cesium levels in Northeast Japan following the Fukushima nuclear accident. Ecotoxicology 25(8):1514–1522
103. Achim P, Monfort M, Le Petit G, Gross P, Douysset G, Taffary T, Blanchard X, Moulin C (2014) Analysis of radionuclide releases from the Fukushima Dai-ichi nuclear power plant accident part II. Pure Appl Geophys 171(3–5):645–667
104. Draxler R, Arnold D, Chino M, Galmarini S, Hort M, Jones A, Leadbetter S, Malo A, Maurer C, Rolph G (2015) World Meteorological Organization's model simulations of the radionuclide dispersion and deposition from the Fukushima Daiichi nuclear power plant accident. J Environ Radioact 139:172–184
105. Lee H-J, Jo H-Y, Nam K-P, Lee K-H, Kim C-H (2017) Measurement, simulation, and meteorological interpretation of medium-range transport of radionuclides to Korea during the Fukushima Dai-ichi nuclear accident. Ann Nucl Energy 103:412–423
106. Tsumune D, Tsubono T, Aoyama M, Hirose K (2012) Distribution of oceanic 137Cs from the Fukushima Dai-ichi nuclear power plant simulated numerically by a regional ocean model. J Environ Radioact 111:100–108
107. Tsumune D, Tsubono T, Aoyama M, Uematsu M, Misumi K, Maeda Y, Yoshida Y, Hayami H (2013) One-year, regional-scale simulation of 137Cs radioactivity in the ocean following the Fukushima Dai-ichi nuclear power plant accident. Biogeosciences 10(8):5601
108. Miyazawa Y, Masumoto Y, Varlamov S, Miyama T, Takigawa M, Honda M, Saino T (2013) Inverse estimation of source parameters of oceanic radioactivity dispersion models associated with the Fukushima accident. Biogeosciences 10(4):2349–2363
109. Saito K, Tanihata I, Fujiwara M, Saito T, Shimoura S, Otsuka T, Onda Y, Hoshi M, Ikeuchi Y, Takahashi F (2015) Detailed deposition density maps constructed by large-scale soil sampling for gamma-ray emitting radioactive nuclides from the Fukushima Dai-ichi nuclear power plant accident. J Environ Radioact 139:308–319
110. Povinec P, Sýkora I, Holý K, Gera M, Kováčik A, Brest'áková L (2012) Aerosol radioactivity record in Bratislava/Slovakia following the Fukushima accident–A comparison with global fallout and the Chernobyl accident. J Environ Radioact 114:81–88
111. Lelieveld J, Lawrence MG, Kunkel D (2012) Global risk of radioactive fallout after major nuclear reactor accidents" by Lelieveld et al. (2012). Atmos Chem Phys 13(1):31–34. https://doi.org/10.5194/acp-13-31-2013
112. Niksarlioglu S, Kulahci F, Sen Z (2015) Spatiotemporal modeling and simulation of chernobyl radioactive fallout in northern Turkey. J Radioanal Nucl Chem 303(1):171–186. https://doi.org/10.1007/s10967-014-3517-z
113. Tanarhte M, Hadjinicolaou P, Lelieveld J (2012) Intercomparison of temperature and precipitation data sets based on observations in the Mediterranean and the Middle East. J Geophys Res Atmos 117(D12):D12102. https://doi.org/10.1029/2011JD017293
114. Thakur P, Ballard S, Nelson R (2013) An overview of Fukushima radionuclides measured in the northern hemisphere. Sci Total Environ 458:577–613. https://doi.org/10.1016/j.scitotenv.2013.03.105
115. Nakanishi TM (2017) Research with radiation and radioisotopes to better understand plant physiology and agricultural consequences of radioactive contamination from the Fukushima Daiichi nuclear accident. J Radioanal Nucl Chem 311(2):947–971. https://doi.org/10.1007/s10967-016-5148-z
116. Ishida M, Yamazaki H (2017) Radioactive contamination in the Tokyo metropolitan area in the early stage of the Fukushima Daiichi nuclear power plant (FDNPP) accident and its fluctuation over five years. PLoS ONE 12(11):e0187687
117. Tanaka K, Iwatani H, Sakaguchi A, Takahashi Y, Onda Y (2013) Local distribution of radioactivity in tree leaves contaminated by fallout of the radionuclides emitted from the Fukushima Daiichi nuclear power plant. J Radioanal Nucl Chem 295(3):2007–2014. https://doi.org/10.1007/s10967-012-2192-1
118. Tanaka K, Sakaguchi A, Kanai Y, Tsuruta H, Shinohara A, Takahashi Y (2013) Heterogeneous distribution of radiocesium in aerosols, soil and particulate matters emitted by the Fukushima Daiichi nuclear power plant accident: retention of micro-scale heterogeneity during the migration of radiocesium from the air into ground and river systems. J Radioanal Nucl Chem 295(3):1927–1937. https://doi.org/10.1007/s10967-012-2160-9
119. Zheng J, Tagami K, Uchida S (2012) Rapid analysis of U isotopes in vegetables using ICP-MS: application to the emergency U monitoring after the nuclear accident at TEPCO's Fukushima Dai-ichi power station. J Radioanal Nucl Chem 292(1):171–175. https://doi.org/10.1007/s10967-011-1387-1
120. Koarashi J, Atarashi-Andoh M, Amano H, Matsunaga T (2017) Vertical distributions of global fallout Cs-137 and C-14 in a Japanese forest soil profile and their implications for the fate and migration processes of Fukushima-derived Cs-137. J Radioanal Nucl Chem 311(1):473–481. https://doi.org/10.1007/s10967-016-4938-7
121. Nihei N, Tanoi K, Nakanishi TM (2016) Monitoring inspection for radiocesium in agricultural, livestock, forestry and fishery products in Fukushima prefecture. J Radioanal Nucl Chem 307(3):2217–2220. https://doi.org/10.1007/s10967-015-4448-z
122. Igarashi Y, Fujiwara H, Jugder D (2011) Change of the Asian dust source region deduced from the composition of anthropogenic radionuclides in surface soil in Mongolia. Atmos Chem Phys 11(14):7069–7080
123. Kusakabe M, Oikawa S, Takata H, Misonoo J (2013) Spatiotemporal distributions of Fukushima-derived radionuclides in nearby marine surface sediments. Biogeosciences 10(7):5019
124. Xu S, Cook GT, Cresswell AJ, Dunbar E, Freeman S, Hou XL, Kinch H, Naysmith P, Sanderson DWC, Zhang LY (2016) Carbon, cesium and iodine isotopes in Japanese cedar leaves from

Iwaki, Fukushima. J Radioanal Nucl Chem 310(2):927–934. https://doi.org/10.1007/s10967-016-4830-5
125. Zhang WH, Friese J, Ungar K (2013) The ambient gamma dose-rate and the inventory of fission products estimations with the soil samples collected at Canadian embassy in Tokyo during Fukushima nuclear accident. J Radioanal Nucl Chem 296(1):69–73. https://doi.org/10.1007/s10967-012-2040-3
126. Koo Y-H, Yang Y-S, Song K-W (2014) Radioactivity release from the Fukushima accident and its consequences: a review. Prog Nucl Energy 74:61–70
127. Pignalberi A, Pezzopane M, Rizzi R, Galkin I (2018) Effective solar indices for ionospheric modeling: a review and a proposal for a real-time regional IRI. Surv Geophys 39(1):125–167. https://doi.org/10.1007/s10712-017-9438-y
128. Cressie N (1990) The origins of kriging. Math Geol 22(3):239–252
129. Olea RA (2017) Resampling of spatially correlated data with preferential sampling for the estimation of frequency distributions and semivariograms. Stoch Environ Res Risk Assess 31(2):481–491. https://doi.org/10.1007/s00477-016-1289-4
130. Krige DG (1951) A statistical approach to some basic mine valuation problems on the Witwatersrand. J S Afr Inst Min Metall 52(6):119–139
131. Matheron G (1963) Principles of geostatistics. Econ Geol 58(8):1246–1266. https://doi.org/10.2113/gsecongeo.58.8.1246
132. Kulahci F (2016) Spatiotemporal (four-dimensional) modeling and simulation of uranium (238) in Hazar Lake (Turkey) water. Environ Earth Sci 75(6):452. https://doi.org/10.1007/s12665-016-5302-5
133. Külahci F (2011) A risk analysis model for radioactive wastes. J Hazard Mater 191(1–3):349–355. https://doi.org/10.1016/j.jhazmat.2011.04.083
134. Külahcı F (2016) Proposals for risk assessment of major cations in surface water and deep sediment: iso-cation curves, probabilities of occurrence and non-occurrence of cations. Environ Earth Sci 75(11):980. https://doi.org/10.1007/s12665-016-5788-x
135. Külahcı F (2016) Spatiotemporal (four-dimensional) modeling and simulation of uranium (238) in Hazar Lake (Turkey) water. Environ Earth Sci 75(6):452. https://doi.org/10.1007/s12665-016-5302-5
136. Kulahci F, Sen Z (2014) On the correction of spatial and statistical uncertainties in systematic measurements of Rn-222 for earthquake prediction. Surv Geophys 35(2):449–478. https://doi.org/10.1007/s10712-013-9273-8
137. Külahci F, Sen Z (2010) Progresses in radioactive contamination researches. In: Radioactive contamination research developments. Nova Science Publishers Inc, Hauppauge, pp 1–42
138. Külahci F, Şen Z (2007) Spatial dispersion modeling of 90Sr by point cumulative semivariogram at Keban Dam Lake, Turkey. Appl Radiat Isotop 65(9):1070–1077. https://doi.org/10.1016/j.apradiso.2007.03.012
139. Külahcı F, Şen Z (2009) Potential utilization of the absolute point cumulative semivariogram technique for the evaluation of distribution coefficient. J Hazard Mater 168(2–3):1387–1396. https://doi.org/10.1016/j.jhazmat.2009.03.027
140. Külahcı F, Şen Z (2009) Spatio-temporal modeling of 210 Pb transportation in lake environments. J Hazard Mater 165(1):525–532
141. Külahcı F, Şen Z, Kazanç S (2008) Cesium concentration spatial distribution modeling by point cumulative semivariogram. Water Air Soil Pollut 195(1–4):151–160. https://doi.org/10.1007/s11270-008-9734-8
142. Şen Z (1989) Cumulative semivariogram models of regionalized variables. Math Geol 21(8):891–903. https://doi.org/10.1007/BF00894454
143. Şen Z (1992) Standard cumulative semivariograms of stationary stochastic processes and regional correlation. Math Geol 24(4):417–435. https://doi.org/10.1007/BF00891272
144. Şen Z (1998) Point cumulative semivariogram for identification of heterogeneities in regional seismicity of Turkey. Math Geol 30(7):767–787. https://doi.org/10.1023/a:1021704507596
145. Şen Z (2009) Spatial modeling principles in Earth sciences. Springer, Berlin
146. Senior C, Blanc M (1984) On the control of magnetospheric convection by the spatial distribution of ionospheric conductivities. J Geophys Res 89(A1):261–284
147. Tallaksen LM, Stahl K (2014) Spatial and temporal patterns of large-scale droughts in Europe: model dispersion and performance. Geophys Res Lett 41(2):2013GL058573. https://doi.org/10.1002/2013gl058573
148. Khan AA, Farid A, Akhter G, Munir K, Small J, Ahmad Z (2016) Geomorphology of the alluvial sediments and bedrock in an intermontane basin: application of variogram modeling to electrical resistivity soundings. Surv Geophys 37(3):579–599. https://doi.org/10.1007/s10712-016-9364-4
149. Külahci F, Şen Z (2014) On the correction of spatial and statistical uncertainties in systematic measurements of 222Rn for earthquake prediction. Surv Geophys 35(2):449–478. https://doi.org/10.1007/s10712-013-9273-8
150. August JK (2011) Fukushima exposes the risks of LWRs. Nucl Eng Int 56(684):16
151. Brombacher A (2011) Fukushima; about risks, reliability and robust design. Qual Reliab Eng Int 27(4):389. https://doi.org/10.1002/qre.1219
152. Butler D (2011) Fukushima health risks scrutinized. Nature 472(7341):13–14. https://doi.org/10.1038/472013a
153. Calabrese E (2011) Improving the scientific foundations for estimating health risks from the Fukushima incident. Proc Natl Acad Sci USA 108(49):19447–19448. https://doi.org/10.1073/pnas.1117296108
154. Lyman ES (2011) Surviving the one-two nuclear punch: assessing risk and policy in a post-Fukushima world. Bull Atom Sci 67(5):47–54. https://doi.org/10.1177/0096340211421470
155. Tanaka HL, Nohara D, Yokoi M (2000) Numerical simulation of wind hole circulation and summertime ice formation at Ice Valley in Korea and Nakayama in Fukushima, Japan. J Meteorol Soc Jpn 78(5):611–630. https://doi.org/10.2151/jmsj1965.78.5_611
156. Prants SV, Uleysky MY, Budyansky MV (2011) Numerical simulation of propagation of radioactive pollution in the ocean from the Fukushima Dai-ichi nuclear power plant. Dokl Earth Sci 439(2):1179–1182. https://doi.org/10.1134/s1028334x11080277
157. Takemura T, Nakamura H, Takigawa M, Kondo H, Satomura T, Miyasaka T, Nakajima T (2011) A numerical simulation of global transport of atmospheric particles emitted from the Fukushima Daiichi nuclear power plant. Sola 7:101–104. https://doi.org/10.2151/sola.2011-026
158. Behrens E, Schwarzkopf FU, Lubbecke JF, Boning CW (2012) Model simulations on the long-term dispersal of Cs-137 released into the Pacific Ocean off Fukushima. Environ Res Lett 7(3):10. https://doi.org/10.1088/1748-9326/7/3/034004
159. Danielache SO, Yoshikawa C, Priyadarshi A, Takemura T, Ueno Y, Thiemens MH, Yoshidai N (2012) An estimation of the radioactive S-35 emitted into the atmospheric from the Fukushima Daiichi nuclear power plant by using a numerical simulation global transport. Geochem J 46(4):335–339
160. Masumoto Y, Miyazawa Y, Tsumune D, Tsubono T, Kobayashi T, Kawamura H, Estournel C, Marsaleix P, Lanerolle L, Mehra A, Garraffos ZD (2012) Oceanic dispersion simulations of Cs-137 released from the Fukushima Daiichi nuclear power plant. Elements 8(3):207–212. https://doi.org/10.2113/gselements.8.3.207

161. Miyazawa Y, Masumoto Y, Varlamov SM, Miyama T (2012) Transport simulation of the radionuclide from the shelf to open ocean around Fukushima. Cont Shelf Res 50–51:16–29. https://doi.org/10.1016/j.csr.2012.09.002
162. Patil S, Chintamani S, Kumar R, Kumar R, Dennis BH, Asme (2016) Numerical analysis of transient temperature distribution in a partially cooled nuclear fuel rod. In: Proceedings of the ASME international mechanical engineering congress and exposition, 2015, vol 8a
163. Hong S, Bradshaw CJA, Brook BW (2013) Evaluating options for the future energy mix of Japan after the Fukushima nuclear crisis. Energy Policy 56:418–424. https://doi.org/10.1016/j.enpol.2013.01.002
164. Poinssot C, Bourg S, Ouvrier N, Combernoux N, Rostaing C, Vargas-Gonzalez M, Bruno J (2014) Assessment of the environmental footprint of nuclear energy systems. Comparison between closed and open fuel cycles. Energy 69:199–211. https://doi.org/10.1016/j.energy.2014.02.069
165. Rodriguez-Penalonga L, Soria BYM (2017) A review of the nuclear fuel cycle strategies and the spent nuclear fuel management technologies. Energies 10(8):1235. https://doi.org/10.3390/en10081235
166. Stamford L, Azapagic A (2014) Life cycle sustainability assessment of UK electricity scenarios to 2070. Energy Sustain Dev 23:194–211. https://doi.org/10.1016/j.esd.2014.09.008
167. Ilg P, Gabbert S, Weikard HP (2017) Nuclear waste management under approaching disaster: a comparison of decommissioning strategies for the German Repository Asse II. Risk Anal 37(7):1213–1232. https://doi.org/10.1111/risa.12648
168. Tanoi K, Uchida K, Doi C, Nihei N, Hirose A, Kobayashi NI, Sugita R, Nobori T, Nakanishi TM, Kanno M, Wakabayashi I, Ogawa M, Tao Y (2016) Investigation of radiocesium distribution in organs of wild boar grown in Iitate, Fukushima after the Fukushima Daiichi nuclear power plant accident. J Radioanal Nucl Chem 307(1):741–746. https://doi.org/10.1007/s10967-015-4233-z
169. Ioannidou A, Manolopoulou EM, Stoulos S, Vagena E, Papastefanou C, Bonardi ML, Gini L, Manenti S, Groppi F (2014) Radionuclides from Fukushima accident in Thessaloniki, Greece (40A degrees N) and Milano, Italy (45A degrees). J Radioanal Nucl Chem 299(1):855–860. https://doi.org/10.1007/s10967-013-2709-2
170. Povinec PP, Sykora I, Gera M, Holy K, Brest'akova L, Kovacik A (2013) Fukushima-derived radionuclides in ground-level air of Central Europe: a comparison with simulated forward and backward trajectories. J Radioanal Nucl Chem 295(2):1171–1176. https://doi.org/10.1007/s10967-012-1943-3
171. Lee SH, Heo DH, Kang HB, Oh PJ, Lee JM, Park TS, Lee KB, Oh JS, Suh JK (2013) Distribution of I-131, Cs-134, Cs-137 and Pu-239, Pu-240 concentrations in Korean rainwater after the Fukushima nuclear power plant accident. J Radioanal Nucl Chem 296(2):727–731. https://doi.org/10.1007/s10967-012-2030-5
172. Thakur P, Ballard S, Nelson R (2012) Radioactive fallout in the United States due to the Fukushima nuclear plant accident. J Environ Monit 14(5):1317–1324. https://doi.org/10.1039/c2em11011c
173. Chang Z, Moore WS, McCullough KD, Morenikeji S (2013) Detection and quantification of gaseous and particulate fukushima fission products at Orangeburg, South Carolina. Health Phys 105(1):49–64. https://doi.org/10.1097/HP.0b013e31828a8f69
174. Kitto ME, Menia TA, Haines DK, Beach SE, Bradt CJ, Fielman EM, Syed UF, Semkow TM, Bari A, Khan AJ (2013) Airborne gamma-ray emitters from Fukushima detected in New York State. J Radioanal Nucl Chem 296(1):49–56. https://doi.org/10.1007/s10967-012-2043-0
175. Tumey SJ, Guilderson TP, Brown TA, Broek T, Buesseler KO (2013) Input of I-129 into the western Pacific Ocean resulting from the Fukushima nuclear event. J Radioanal Nucl Chem 296(2):957–962. https://doi.org/10.1007/s10967-012-2217-9
176. Shrivastava R, Oza RB (2017) Estimation of scavenging coefficients for I-131 and Cs-137 over the Pacific Ocean following the Fukushima accident. Prog Nucl Energy 98:228–233. https://doi.org/10.1016/j.pnucene.2017.03.026
177. Chester A, Starosta K, Andreoiu C, Ashley R, Barton A, Brodovitch JC, Brown M, Domingo T, Janusson C, Kucera H, Myrtle K, Riddell D, Scheel K, Salomon A, Voss P (2013) Monitoring rainwater and seaweed reveals the presence of I-131 in southwest and central British Columbia, Canada following the Fukushima nuclear accident in Japan. J Environ Radioact 124:205–213. https://doi.org/10.1016/j.jenvrad.2013.05.013
178. Potiriadis C, Kolovou M, Clouvas A, Xanthos S (2012) Environmental radioactivity measurements in Greece following the Fukushima Daichi nuclear accident. Radiat Prot Dosimet 150(4):441–447. https://doi.org/10.1093/rpd/ncr423
179. Parache V, Pourcelot L, Roussel-Debet S, Orjollet D, Leblanc F, Soria C, Gurriaran R, Renaud P, Masson O (2011) Transfer of I-131 from Fukushima to the vegetation and milk in France. Environ Sci Technol 45(23):9998–10003. https://doi.org/10.1021/es202242g
180. Perrot F, Hubert P, Marquet C, Pravikoff MS, Bourquin P, Chiron H, Guernion PY, Nachab A (2012) Evidence of I-131 and (CS)-C-134,137 activities in Bordeaux, France due to the Fukushima nuclear accident. J Environ Radioact 114:61–65. https://doi.org/10.1016/j.jenvrad.2011.12.026
181. Masson O, Ringer W, Mala H, Rulik P, Dlugosz-Lisiecka M, Eleftheriadis K, Meisenberg O, De Vismes-Ott A, Gensdarmes F (2013) Size distributions of airborne radionuclides from the Fukushima Nuclear Accident at several places in Europe. Environ Sci Technol 47(19):10995–11003. https://doi.org/10.1021/es401973c
182. Lopez-Perez M, Ramos-Lopez R, Perestelo NR, Duarte-Rodriguez X, Bustos JJ, Alonso-Perez S, Cuevas E, Hernandez-Armas J (2013) Arrival of radionuclides released by the Fukushima accident to Tenerife (Canary Islands). J Environ Radioact 116:180–186. https://doi.org/10.1016/j.jenvrad.2012.09.011
183. Bihari A, Dezso Z, Bujtas T, Manga L, Lencses A, Dombovari P, Csige I, Ranga T, Mogyorosi M, Veres M (2014) Fission products from the damaged Fukushima reactor observed in Hungary. Isotop Environ Health Stud 50(1):94–102. https://doi.org/10.1080/10256016.2013.828717
184. Masson O, Bieringer J, Brattich E, Dalheimer A, Estier S, Penev I, Ringer W, Schlosser C, Steinkopff T, Steinmann P, Tositti L, Van Beek P, de Vismes-Ott A (2016) Variation in airborne Cs-134, Cs-137, particulate I-131 and Be-7 maximum activities at high-altitude European locations after the arrival of Fukushima-labeled air masses. J Environ Radioact 162:14–22. https://doi.org/10.1016/j.jenvrad.2016.05.004
185. Beresford NA, Barnett CL, Howard BJ, Howard DC, Wells C, Tyler AN, Bradley S, Copplestone D (2012) Observations of Fukushima fallout in Great Britain. J Environ Radioact 114:48–53. https://doi.org/10.1016/j.jenvrad.2011.12.008
186. Carvalho FP, Reis MC, Oliveira JM, Malta M, Silva L (2012) Radioactivity from Fukushima nuclear accident detected in Lisbon, Portugal. J Environ Radioact 114:152–156. https://doi.org/10.1016/j.jenvrad.2012.03.005
187. Cosma C, Iurian AR, Nita DC, Begy R, Cindea C (2012) Indicators of the Fukushima radioactive release in NW Romania. J Environ Radioact 114:94–99. https://doi.org/10.1016/j.jenvrad.2011.11.020
188. Gudelis A, Druteikiene R, Lujaniene G, Maceika E, Plukis A, Remeikis V (2012) Radionuclides in the ground-level

atmosphere in Vilnius, Lithuania, in March 2011, detected by gamma-ray spectrometry. J Environ Radioact 109:13–18. https://doi.org/10.1016/j.jenvrad.2011.12.021
189. Huh CA, Hsu SC, Lin CY (2012) Fukushima-derived fission nuclides monitored around Taiwan: free tropospheric versus boundary layer transport. Earth Planet Sci Lett 319:9–14. https://doi.org/10.1016/j.epsl.2011.12.004
190. Ioannidou A, Manenti S, Gini L, Groppi F (2012) Fukushima fallout at Milano, Italy. J Environ Radioact 114:119–125. https://doi.org/10.1016/j.jenvrad.2012.01.006
191. Long NQ, Truong Y, Hien PD, Binh NT, Sieu LN, Giap TV, Phan NT (2012) Atmospheric radionuclides from the Fukushima Dai-ichi nuclear reactor accident observed in Vietnam. J Environ Radioact 111:53–58. https://doi.org/10.1016/j.jenvrad.2011.11.018
192. Matsui T (2011) Deciphering the measured ratios of iodine-131 to cesium-137 at the Fukushima reactors. Prog Theor Phys 126(6):1167–1176. https://doi.org/10.1143/ptp.126.1167
193. Kamada N, Saito O, Endo S, Kimura A, Shizuma K (2012) Radiation doses among residents living 37 km northwest of the Fukushima Dai-ichi nuclear power plant. J Environ Radioact 110:84–89. https://doi.org/10.1016/j.jenvrad.2012.02.007
194. Landis JD, Hamm NT, Renshaw CE, Dade WB, Magilligan FJ, Gartner JD (2012) Surficial redistribution of fallout (131) iodine in a small temperate catchment. Proc Natl Acad Sci USA 109(11):4064–4069. https://doi.org/10.1073/pnas.1118665109
195. Yamauchi M (2012) Secondary wind transport of radioactive materials after the Fukushima accident. Earth Planets Space 64(1):E1–E4. https://doi.org/10.5047/eps.2012.01.002
196. MEXT JMoE, culture, sports, science and technology MEXT, Japan Ministry of Education, Culture, Sports, Science and Technology. http://www.mext.go.jp/en/incident/title01/detail01/sdetail01/1373008.htm. Accessed 1 Jan 2019
197. Kosaka K, Asami M, Kobashigawa N, Ohkubo K, Teracia H, Kishicla N, Akiba M (2012) Removal of radioactive iodine and cesium in water purification processes after an explosion at a nuclear power plant due to the Great East Japan Earthquake. Water Res 46(14):4397–4404. https://doi.org/10.1016/j.watres.2012.05.055
198. Higaki S, Hirota M (2012) Decontamination efficiencies of pot-type water purifiers for I-131, Cs-134 and Cs-137 in rainwater contaminated during Fukushima Daiichi Nuclear Disaster. PLoS ONE 7(5):4. https://doi.org/10.1371/journal.pone.0037184
199. Mallampati SR, Mitoma Y, Okuda T, Sakita S, Kakeda M (2012) High immobilization of soil cesium using ball milling with nano-metallic Ca/CaO/NaH_2PO_4: implications for the remediation of radioactive soils. Environ Chem Lett 10(2):201–207. https://doi.org/10.1007/s10311-012-0357-3
200. Murakami M, Oki T (2012) Estimation of thyroid doses and health risks resulting from the intake of radioactive iodine in foods and drinking water by the citizens of Tokyo after the Fukushima nuclear accident. Chemosphere 87(11):1355–1360. https://doi.org/10.1016/j.chemosphere.2012.02.028
201. Tanaka K, Takahashi Y, Sakaguchi A, Umeo M, Hayakawa S, Tanida H, Saito T, Kanai Y (2012) Vertical profiles of iodine-131 and cesium-137 in soils in Fukushima prefecture related to the Fukushima Daiichi Nuclear Power Station Accident. Geochem J 46(1):73–76
202. Ohno T, Muramatsu Y, Miura Y, Oda K, Inagawa N, Ogawa H, Yamazaki A, Toyama C, Sato M (2012) Depth profiles of radioactive cesium and iodine released from the Fukushima Daiichi nuclear power plant in different agricultural fields and forests. Geochem J 46(4):287–295
203. Honda M, Matsuzaki H, Miyake Y, Maejima Y, Yamagata T, Nagai H (2015) Depth profile and mobility of I-129 and Cs-137 in soil originating from the Fukushima Dai-ichi nuclear power plant accident. J Environ Radioact 146:35–43. https://doi.org/10.1016/j.jenvrad.2015.03.029
204. Imanaka T, Hayashi G, Endo S (2015) Comparison of the accident process, radioactivity release and ground contamination between Chernobyl and Fukushima-1. J Radiat Res 56:I56–I61. https://doi.org/10.1093/jrr/rrv074
205. Matsunaka T, Sasa K, Sueki K, Takahashi T, Matsumura M, Satou Y, Kitagawa J, Kinoshita N, Matsuzaki H (2015) Post-accident response of near-surface I-129 levels and I-129/I-127 ratios in areas close to the Fukushima Dai-ichi nuclear power plant, Japan. Nucl Instrum Methods Phys Res Sect B Beam Interact Mater Atoms 361:569–573. https://doi.org/10.1016/j.nimb.2015.03.056
206. Matsunaka T, Sasa K, Sueki K, Takahashi T, Satou Y, Matsumura M, Kinoshita N, Kitagawa JI, Matsuzaki H (2016) Pre- and post-accident I-129 and Cs-137 levels, and I-129/Cs-137 ratios in soil near the Fukushima Dai-ichi nuclear power plant, Japan. J Environ Radioact 151:209–217. https://doi.org/10.1016/j.jenvrad.2015.10.010
207. Honda M, Matsuzaki H, Nagai H, Sueki K (2017) Depth profiles and mobility of I-129 originating from the Fukushima Dai-ichi nuclear power plant disaster under different land uses. Appl Geochem 85:169–179. https://doi.org/10.1016/j.apgeochem.2017.01.023
208. Miyake Y, Matsuzaki H, Fujiwara T, Saito T, Yamagata T, Honda M, Muramatsu Y (2012) Isotopic ratio of radioactive iodine (I-129/I-131) released from Fukushima Daiichi NPP accident. Geochem J 46(4):327–333
209. Fujiwara H (2016) Observation of radioactive iodine (I-131, I-129) in cropland soil after the Fukushima nuclear accident. Sci Total Environ 566:1432–1439. https://doi.org/10.1016/j.scitotenv.2016.06.004
210. Daraoui A, Riebe B, Walther C, Wershofen H, Schlosser C, Vockenhuber C, Synal HA (2016) Concentrations of iodine isotopes (I-129 and I-127) and their isotopic ratios in aerosol samples from Northern Germany. J Environ Radioact 154:101–108. https://doi.org/10.1016/j.jenvrad.2016.01.021
211. Yoshida N, Takahashi Y (2012) Land-surface contamination by radionuclides from the Fukushima Daiichi nuclear power plant accident. Elements 8(3):201–206. https://doi.org/10.2113/gselements.8.3.201
212. Park SU, Lee IH, Ju JW, Joo SJ (2016) Estimation of radionuclide (137Cs) emission rates from a nuclear power plant accident using the Lagrangian particle dispersion model (LPDM). J Environ Radioact 162–163:258–262. https://doi.org/10.1016/j.jenvrad.2016.05.033
213. Liu Y, Haussaire JM, Bocquet M, Roustan Y, Saunier O, Mathieu A (2017) Uncertainty quantification of pollutant source retrieval: comparison of Bayesian methods with application to the Chernobyl and Fukushima Daiichi accidental releases of radionuclides. Q J R Meteorol Soc 143(708):2886–2901. https://doi.org/10.1002/qj.3138
214. Woo TH (2013) Atmospheric modeling of radioactive material dispersion and health risk in Fukushima Daiichi nuclear power plants accident. Ann Nucl Energy 53:197–201. https://doi.org/10.1016/j.anucene.2012.09.003
215. Guan Y, Shen SF, Huang H (2015) The numerical simulation of caesium-137 transportation in ocean and the assessment of its radioactive impacts after Fukushima NPP release. Sci China-Earth Sci 58(6):996–1004. https://doi.org/10.1007/s11430-014-5032-z
216. Rafindadi AA, Ozturk I (2016) Effects of financial development, economic growth and trade on electricity consumption: evidence from post-Fukushima Japan. Renew Sustain Energ Rev 54:1073–1084. https://doi.org/10.1016/j.rser.2015.10.023
217. Schoppner M, Plastino W, Povinec PP, Wotawa G, Bella F, Budano A, De Vincenzi M, Ruggieri F (2012) Estimation of

the time-dependent radioactive source-term from the Fukushima nuclear power plant accident using atmospheric transport modelling. J Environ Radioact 114:10–14. https://doi.org/10.1016/j.jenvrad.2011.11.008

218. Rulik P, Hyza M, Beckova V, Borecky Z, Havranek J, Holgye Z, Lusnak J, Mala H, Matzner J, Pilatova H, Rada J, Schlesingerova E, Sindelkova E, Dragounova L, Vlcek J (2015) Monitoring radionuclides in the atmosphere over the Czech Republic after the Fukushima nuclear power plant accident. Radiat Prot Dosimet 163(2):226–232. https://doi.org/10.1093/rpd/ncu154
219. Saunier O, Mathieu A, Didier D, Tombette M, Quélo D, Winiarek V, Bocquet M (2012) Using gamma dose rate monitoring with inverse modeling techniques to estimate the atmospheric release of a nuclear power plant accident: application to the Fukushima case. In: Proc. Int. international meeting on severe accident assessment and management: lessons learned from Fukushima Dai-ichi, San Diego, California, pp 422–429
220. Winiarek V, Bocquet M, Saunier O, Mathieu A (2012) Estimation of errors in the inverse modeling of accidental release of atmospheric pollutant: application to the reconstruction of the cesium-137 and iodine-131 source terms from the Fukushima Daiichi power plant (vol 117, D18118, 2012). J Geophys Res-Atmos 117:2. https://doi.org/10.1029/2012jd018107
221. Leelossy A, Lagzi I, Kovacs A, Meszaros R (2018) A review of numerical models to predict the atmospheric dispersion of radionuclides. J Environ Radioact 182:20–33. https://doi.org/10.1016/j.jenvrad.2017.11.009
222. Wang J, Brown DG, Hammerling D (2013) Geostatistical inverse modeling for super-resolution mapping of continuous spatial processes. Remote Sens Environ 139:205–215. https://doi.org/10.1016/j.rse.2013.08.007
223. Sharma LK, Ghosh AK, Nair RN, Chopra M, Sunny F, Puranik VD (2014) Inverse modeling for aquatic source and transport parameters identification and its application to Fukushima nuclear accident. Environ Model Assess 19(3):193–206. https://doi.org/10.1007/s10666-013-9391-1
224. Babukhina TI, Gan'shin AV, Zhuravlev RV, Luk'yanov AN, Maksyutov SS (2016) Estimating by inverse modeling the release of radioactive substances (133Xe, 131I, and 137Cs) into the atmosphere from Fukushima Daiichi nuclear disaster. Russ Meteorol Hydrol 41(5):335–343. https://doi.org/10.3103/S1068373916050046
225. Göckede M, Michalak AM, Vickers D, Turner DP, Law BE (2010) Atmospheric inverse modeling to constrain regional-scale CO_2 budgets at high spatial and temporal resolution. J Geophys Res Atmos 115(D15):D15113. https://doi.org/10.1029/2009JD012257
226. Estournel C, Bosc E, Bocquet M, Ulses C, Marsaleix P, Winiarek V, Osvath I, Nguyen C, Duhaut T, Lyard F, Michaud H, Auclair F (2012) Assessment of the amount of cesium-137 released into the Pacific Ocean after the Fukushima accident and analysis of its dispersion in Japanese coastal waters. J Geophys Res: Oceans. https://doi.org/10.1029/2012jc007933
227. Lamego Simões Filho FF, Duarte Soares A, Da Silva Aguiar A, Franklin Lapa CM, Ferreira Guimarães AC (2013) Advanced nuclear reactors and tritium impacts. Modeling the aquatic pathway. Prog Nucl Energy 69:9–22. https://doi.org/10.1016/j.pnucene.2013.02.002
228. Yumimoto K, Morino Y, Ohara T, Oura Y, Ebihara M, Tsuruta H, Nakajima T (2016) Inverse modeling of the 137Cs source term of the Fukushima Dai-ichi nuclear power plant accident constrained by a deposition map monitored by aircraft. J Environ Radioact 164:1–12. https://doi.org/10.1016/j.jenvrad.2016.06.018
229. Leelőssy Á, Lagzi I, Kovács A, Mészáros R (2018) A review of numerical models to predict the atmospheric dispersion of radionuclides. J Environ Radioact 182:20–33. https://doi.org/10.1016/j.jenvrad.2017.11.009
230. Zhang X, Raskob W, Landman C, Trybushnyi D, Haller C, Yuan H (2017) Automatic plume episode identification and cloud shine reconstruction method for ambient gamma dose rates during nuclear accidents. J Environ Radioact 178–179:36–47. https://doi.org/10.1016/j.jenvrad.2017.07.014
231. Krysta M, Bocquet M (2007) Source reconstruction of an accidental radionuclide release at European scale. Q J R Meteorol Soc 133(623):529–544. https://doi.org/10.1002/qj.3
232. Zhang ZJ, Ninomiya K, Takahashi N, Shinohara A (2015) Daily variation of I-131, Cs-134 and Cs-137 activity concentrations in the atmosphere in Osaka during the early phase after the FDNPP accident. J Radioanal Nucl Chem 303(2):1527–1531. https://doi.org/10.1007/s10967-014-3752-3
233. Terasaka Y, Yamazawa H, Hirouchi J, Hirao S, Sugiura H, Moriizumi J, Kuwahara Y (2016) Air concentration estimation of radionuclides discharged from Fukushima Daiichi Nuclear Power Station using NaI(Tl) detector pulse height distribution measured in Ibaraki Prefecture. J Nucl Sci Tech 53(12):1919–1932. https://doi.org/10.1080/00223131.2016.1193453
234. Wengle H, van den Bosch B, Seinfeld JH (1978) Solution of atmospheric diffusion problems by pseudo-spectral and orthogonal collocation methods. Atmos Environ A Gen Top 12(5):1021–1032. https://doi.org/10.1016/0004-6981(78)90347-5
235. Brandhoff PN, van Bourgondien MJ, Onstenk CGM, van Avezathe AV, Peters RJB (2016) Operation and performance of a national monitoring network for radioactivity in food. Food Control 64:87–97. https://doi.org/10.1016/j.foodcont.2015.12.008
236. Marzo GA (2014) Atmospheric transport and deposition of radionuclides released after the Fukushima Dai-chi accident and resulting effective dose. Atmos Environ 94:709–722. https://doi.org/10.1016/j.atmosenv.2014.06.009
237. Evangeliou N, Balkanski Y, Cozic A, Møller AP (2014) Global and local cancer risks after the Fukushima nuclear power plant accident as seen from Chernobyl: a modeling study for radiocaesium (134Cs & 137Cs). Environ Int 64:17–27. https://doi.org/10.1016/j.envint.2013.11.020
238. Evangeliou N, Balkanski Y, Cozic A, Møller AP (2014) How "lucky" we are that the Fukushima disaster occurred in early spring. Predictions on the contamination levels from various fission products released from the accident and updates on the risk assessment for solid and thyroid cancers. Sci Total Environ 500–501:155–172. https://doi.org/10.1016/j.scitotenv.2014.08.102
239. Kurihara O, Kim E, Kunishima N, Tani K, Ishikawa T, Furuyama K, Hashimoto S, Akashi M (2017) Development of a tool for calculating early internal doses in the Fukushima Daiichi nuclear power plant accident based on atmospheric dispersion simulation. In: Malvagi F, Malouch F, Diop CMB, Miss J, Trama JC (eds) Icrs-13 & Rpsd-2016, 13th International conference on radiation shielding & 19th Topical meeting of the radiation protection and shielding division of the American Nuclear Society—2016, vol 153. EPJ Web of Conferences. E D P Sciences, Cedex A. https://doi.org/10.1051/epjconf/201715308008
240. Evangeliou N, Hamburger T, Cozic A, Balkanski Y, Stohl A (2017) Inverse modeling of the Chernobyl source term using atmospheric concentration and deposition measurements. Atmos Chem Phys 17(14):8805–8824. https://doi.org/10.5194/acp-17-8805-2017
241. Ashraf MA, Akib S, Maah MJ, Yusoff I, Balkhair KS (2014) Cesium-137: radio-chemistry, fate, and transport, remediation, and future concerns. Crit Rev Environ Sci Technol 44(15):1740–1793. https://doi.org/10.1080/10643389.2013.790753
242. Amano H, Akiyama M, Bi CL, Kawamura T, Kishimoto T, Kuroda T, Muroi T, Odaira T, Ohta Y, Takeda K, Watanabe Y, Morimoto T (2012) Radiation measurements in the Chiba

Metropolitan Area and radiological aspects of fallout from the Fukushima Dai-ichi nuclear power plants accident. J Environ Radioact 111:42–52. https://doi.org/10.1016/j.jenvrad.2011.10.019
243. Kojima S (2014) effect of ionizing radiation on the living body. Yakugaku Zasshi-J Pharm Soc Jpn 134(2):155–161. https://doi.org/10.1248/yakushi.13-00227-4
244. Murakami M, Oki T (2014) Estimated dietary intake of radionuclides and health risks for the citizens of Fukushima City, Tokyo, and Osaka after the 2011 nuclear accident. PLoS ONE 9(11):12. https://doi.org/10.1371/journal.pone.0112791
245. Watanobe H, Furutani T, Nihei M, Sakuma Y, Yanai R, Takahashi M, Sato H, Sagawa F (2014) The thyroid status of children and adolescents in Fukushima prefecture examined during 20–30 months after the Fukushima nuclear power plant disaster: a cross-sectional, observational study. PLoS ONE 9(12):19. https://doi.org/10.1371/journal.pone.0113804
246. Wemeau JL (2015) Thyroid and ionizing radiation. Corresp M H D N 19(8):218–222
247. Reiners C, Schneider R, Akashi M, Akl EA, Jourdain JR, Li C, Murith C, Van Bladel L, Yamashita S, Zeeb H, Vitti P, Carr Z (2016) The first meeting of the WHO guideline development group for the revision of the WHO 1999 guidelines for iodine thyroid blocking. Radiat Prot Dosimet 171(1):47–56. https://doi.org/10.1093/rpd/ncw238
248. El Samad O, Baydoun R, Aoun M, Zaidan W, El Jeaid H (2017) Public exposure to radioactivity levels in the Lebanese environment. Environ Sci Pollut Res 24(2):2010–2018. https://doi.org/10.1007/s11356-016-7911-7
249. Steinhauser G, Chavez-Ortega M, Vahlbruch JW (2017) Japanese food data challenge the claimed link between Fukushima's releases and recently observed thyroid cancer increase in Japan. Sci Rep 7:7. https://doi.org/10.1038/s41598-017-10584-8
250. Yasui S (2017) Tertiary evaluation of the committed effective dose of emergency workers that responded to the Fukushima Daiichi NPP accident. J Occup Environ Hyg 14(6):D69–D79. https://doi.org/10.1080/15459624.2017.1285487
251. Tani K, Kurihara O, Kim E, Yoshida S, Sakai K, Akashi M (2015) Implementation of iodine biokinetic model for interpreting I-131 contamination in breast milk after the Fukushima nuclear disaster. Sci Rep 5:9. https://doi.org/10.1038/srep12426
252. Hosoda M, Tokonami S, Akiba S, Kurihara O, Sorimachi A, Ishikawa T, Momose T, Nakano T, Mariya Y, Kashiwakura I (2013) Estimation of internal exposure of the thyroid to I-131 on the basis of Cs-134 accumulated in the body among evacuees of the Fukushima Daiichi Nuclear Power Station accident. Environ Int 61:73–76. https://doi.org/10.1016/j.envint.2013.09.013
253. Kim E, Kurihara O, Tani K, Ohmachi Y, Fukutsu K, Sakai K, Akashi M (2016) Intake ratio of I-131 to Cs-137 derived from thyroid and whole-body doses to Fukushima residents. Radiat Prot Dosimet 168(3):408–418. https://doi.org/10.1093/rpd/ncv344
254. Steinhauser G, Merz S, Kubber-Heiss A, Katzlberger C (2012) Using animal thyroids as ultra-sensitive biomonitors for environmental radioiodine. Environ Sci Technol 46(23):12890–12894. https://doi.org/10.1021/es303280g
255. Mori T, Akamatsu M, Okamoto K, Sumita M, Tateyama Y, Sakai H, Hill JP, Abe M, Ariga K (2013) Micrometer-level naked-eye detection of caesium particulates in the solid state. Sci Technol Adv Mater 14(1):14. https://doi.org/10.1088/1468-6996/14/1/015002
256. Kurihara O, Nakagawa T, Takada C, Tani K, Kim E, Momose T (2016) Internal doses of three persons staying 110 km south of the fukushima daiichi nuclear power station during the arrivalof radioactive plumes based on direct measurements. Radiat Prot Dosimet 170(1–4):420–424. https://doi.org/10.1093/rpd/ncw002
257. Nagataki S, Takamura N, Kamiya K, Akashi M (2013) Measurements of individual radiation doses in residents living around the Fukushima nuclear power plant. Radiat Res 180(5):439–447. https://doi.org/10.1667/rr13351.1
258. Matsuzaki H, Nakano C, Tsuchiya YS, Ito S, Morita A, Kusuno H, Miyake Y, Honda M, Bautista AT, Kawamoto M, Tokuyama H (2015) The status of the AMS system at MALT in its 20th year. Nucl Instrum Methods Phys Res Sect B Beam Interact Mater Atoms 361:63–68. https://doi.org/10.1016/j.nimb.2015.05.032
259. Torii T, Sugita T, Okada CE, Reed MS, Blumenthal DJ (2013) Enhanced analysis methods to derive the spatial distribution of i-131 deposition on the ground by airborne surveys at an early stage after the fukushima daiichi nuclear power plant accident. Health Phys 105(2):192–200. https://doi.org/10.1097/HP.0b013e318294444e
260. Harvey TF, Shapiro CS, Wittler RF (1992) Fallout risk following a major nuclear attack on the United-States. Health Phys 62(1):16–28. https://doi.org/10.1097/00004032-199201000-00003
261. Hohryakov VF, Syslova CG, Skryabin AM (1994) Plutonium and the risk of cancer—a comparative-analysis of pu-body burdens due to releases from nuclear-plants (chelyabinsk-65, gomel area) and global fallout. Sci Total Environ 142(1–2):101–104. https://doi.org/10.1016/0048-9697(94)90077-9
262. Krivoruchko K (1997) Geostatistical picturing of Chernobyl fallout and estimation of cancer risk among Belarus population. In: Geographical information '97: from research to application through cooperation, vols 1 and 2. IOS Press, Amsterdam
263. Macready N (1997) Nuclear test fallout linked to cancer risk. Br Med J 315(7104):329
264. Nishimura R, Morisawa S, Shimada Y (1998) Evaluation of the Japanese health risks induced by global fallout tritium. Health Phys 75(3):259–268. https://doi.org/10.1097/00004032-199809000-00004
265. Shimada Y, Morisawa S (1998) Uncertainty analysis in estimating Japanese ingestion of global fallout Cs-137 using health risk evaluation model. J At Energy Soc Jpn 40(9):713–722. https://doi.org/10.3327/jaesj.40.713
266. Shimada Y, Morisawa S, Yoneda M, Inoue Y (1998) A dosimetric determination of Cs-137 ingestion from global fallout and the related risks to Japanese. Health Phys 74(3):316–329. https://doi.org/10.1097/00004032-199803000-00004
267. Morisawa S, Kitou M, Shimada Y, Yoneda M (2000) Evaluation of fallout strontium-90 accumulation in bone and cancer mortality risk in Japanese. J At Energy Soc Jpn 42(9):951–959. https://doi.org/10.3327/jaesj.42.951
268. Catelinois O, Laurier D, Verger P, Rogel A, Colonna M, Ignasiak M, Hemon D, Tirmarche M (2005) Uncertainty and sensitivity analysis in assessment of the thyroid cancer risk related to Chernobyl fallout in Eastern France. Risk Anal 25(2):243–252. https://doi.org/10.1111/j.1539-6924.2005.00586.x
269. Simon SL, Bouville A, Land CE (2006) Fallout from nuclear weapons tests and cancer risks—exposures 50 years ago still have health implications today that will continue into the future. Am Sci 94(1):48–57. https://doi.org/10.1511/2006.57.982
270. Land CE, Bouville A, Apostoaei I, Simon SL (2010) Projected lifetime cancer risks from exposure to regional radioactive fallout in the marshall islands. Health Phys 99(2):201–215. https://doi.org/10.1097/HP.0b013e3181dc4e84
271. Simon SL, Bouville A, Land CE, Beck HL (2010) Radiation doses and cancer risks in the Marshall Islands associated with exposure to radioactive fallout from bikini and enewetak nuclear weapons tests: summary. Health Phys 99(2):105–123. https://doi.org/10.1097/HP.0b013e3181dc523c

272. Hazama R, Matsushima A (2013) Measurement of fallout with rain in Hiroshima and several sites in Japan from the Fukushima reactor accident. J Radioanal Nucl Chem 297(3):469–475. https://doi.org/10.1007/s10967-012-2417-3
273. Biass S, Scaini C, Bonadonna C, Folch A, Smith K, Hoskuldsson A (2014) A multi-scale risk assessment for tephra fallout and airborne concentration from multiple Icelandic volcanoes—part 1: hazard assessment. Nat Hazards Earth Syst Sci 14(8):2265–2287. https://doi.org/10.5194/nhess-14-2265-2014
274. Scaini C, Biass S, Galderisi A, Bonadonna C, Folch A, Smith K, Hoskuldsson A (2014) A multi-scale risk assessment for tephra fallout and airborne concentration from multiple Icelandic volcanoes—part 2: vulnerability and impact. Nat Hazards Earth Syst Sci 14(8):2289–2312. https://doi.org/10.5194/nhess-14-2289-2014
275. Cahoon EK, Nadyrov EA, Polyanskaya ON, Yauseyenka VV, Veyalkin IV, Yeudachkova TI, Maskvicheva TI, Minenko VF, Liu W, Drozdovitch V, Mabuchi K, Little MP, Zablotska LB, McConnell RJ, Hatch M, Peters KO, Rozhko AV, Brenner AV (2017) Risk of thyroid nodules in residents of Belarus exposed to chernobyl fallout as children and adolescents. J Clin Endocrinol Metab 102(7):2207–2217. https://doi.org/10.1210/jc.2016-3842
276. Wakeford R (2014) The risk of leukaemia in young children from exposure to tritium and carbon-14 in the discharges of German nuclear power stations and in the fallout from atmospheric nuclear weapons testing. Radiat Environ Biophys 53(2):365–379. https://doi.org/10.1007/s00411-014-0516-y
277. Okuma, Japan 1 WHO: Fukushima caused minimal cancer risk (2013). Science 339(6124):1130–1130
278. Global report on Fukushima nuclear accident details health risks (2013). Wkly Epidemiol Rec 88(10):115–116
279. Risk-communication practice with the public after the fukushima power plant accident; The support and consultation for the proper recognition about radiation and health: Japan atomic energy risk communication study office (2012). Atomosphere 54 (8):543-548
280. Cho TJ, Kim NH, Hong YJ, Park B, Kim HS, Lee HG, Song MK, Rhee MS (2017) Development of an effective tool for risk communication about food safety issues after the Fukushima nuclear accident: what should be considered? Food Control 79:17–26. https://doi.org/10.1016/j.foodcont.2017.03.023
281. Ochiai S, Yamamoto M, Nagao S, Itono T, Kashiwaya K (2015) Sediment transport processes in a reservoir-catchment system inferred from sediment trap observations and fallout radionuclides. J Radioanal Nucl Chem 303(2):1497–1501. https://doi.org/10.1007/s10967-014-3577-0
282. Oikawa S, Watabe T, Takata H, Misonoo J, Kusakabe M (2015) Plutonium isotopes and Am-241 in surface sediments off the coast of the Japanese islands before and soon after the Fukushima Dai-ichi nuclear power plant accident. J Radioanal Nucl Chem 303(2):1513–1518. https://doi.org/10.1007/s10967-014-3530-2
283. Aliyu AS, Ramli AT, Garba NN, Saleh MA, Gabdo HT, Liman MS (2015) Fukushima nuclear accident: preliminary assessment of the risks to non-human biota. Radiat Prot Dosimet 163(2):238–250. https://doi.org/10.1093/rpd/ncu158
284. Barabashev S, Skalozubov V (2012) Radiation impact from the Fukushima-1 accident on the environment and public and assessment of radiological risks from beyond design basis accidents at WWER-1000 NPPs based on Fukushima-1 accident consequences. Nucl Radiat Saf 1(53):10–15
285. Belyakov A (2015) From Chernobyl to Fukushima: an interdisciplinary framework for managing and communicating food security risks after nuclear plant accidents. J Environ Stud Sci 5(3):404–417. https://doi.org/10.1007/s13412-015-0284-2
286. Chi M, Shi LP (2011) Risk communication system: case studies of Fukushima accident, pp 466–473. https://doi.org/10.1109/iscram.2011.6184042
287. Isnard O, Chabanis O, Dubiau P (2012) Local response to the Fukushima Dai-ichi nuclear accident at Tokyo: technical support to the french embassy and risk communication to the French community living in Japan, pp 400–403
288. Hagmann J (2012) Fukushima: probing the analytical and epistemological limits of risk analysis. J Risk Res 15(7):801–815. https://doi.org/10.1080/13669877.2012.657223
289. Kaiser JC (2012) Empirical risk analysis of severe reactor accidents in nuclear power plants after Fukushima. Sci Technol Nucl Install 1:1. https://doi.org/10.1155/2012/384987
290. Kinoshita T (2011) The disaster by the Fukushima nuclear power plants and the risk science. Atomos 53(7):465–472
291. Yamashita S (2011) Fukushima Daiichi nuclear accident and radiation health risk. Atmosphere 53(10):678–683
292. Fujinaga A, Yoneda M, Ikegami M (2013) Risk assessment of the intake of foods and soil with the radionuclides and the air radiation dose after the Fukushima nuclear disaster. American Society of Mechanical Engineers (ASME), New York. https://doi.org/10.1115/icone21-15862
293. Fujinaga A, Yoneda M, Ikegami M (2014) Risk assessment of the intake of foods and soil with the radionuclides and the air radiation dose after the Fukushima nuclear disaster. J Eng Gas Turbines Power-Trans ASME 136(8):7. https://doi.org/10.1115/1.4026811
294. Fujinaga A, Yoneda M, Ikegami M, Asme (2014) Risk assessment of the intake of foods and soil with the radionuclides and the air radiation dose after the fukushima nuclear disaster. In: Proceedings of the 21st international conference on nuclear engineering—2013, vol 1. American Society Mechanical Engineers, New York
295. Yu W, He JH, Lin WH, Li YL, Men W, Wang FF, Huang J (2015) Distribution and risk assessment of radionuclides released by Fukushima nuclear accident at the northwest Pacific. J Environ Radioact 142:54–61. https://doi.org/10.1016/j.jenvrad.2015.01.005
296. Otaki JM (2016) Fukushima's lessons from the blue butterfly: a risk assessment of the human living environment in the post-Fukushima era. Integr Environ Assess Manag 12(4):667–672. https://doi.org/10.1002/ieam.1828
297. Sy MM, Gonze MA, Métivier JM, Nicoulaud-Gouin V, Simon-Cornu M (2016) Uncertainty analysis in post-accidental risk assessment models: an application to the Fukushima accident. Ann Nucl Energy 93:94–106. https://doi.org/10.1016/j.anucene.2015.12.033
298. Yamaguchi A (2017) Perspective of risk assessment and management after 5 years of Fukushima Dai-ichi accident. International Association for Probablistic Safety Assessment and Management (IAPSAM)
299. Yamaguchi A, Jang S, Hida K, Yamanaka Y, Narumiya Y (2017) Risk assessment strategy for decommissioning of Fukushima Daiichi nuclear power station. Nucl Eng Technol 49(2):442–449. https://doi.org/10.1016/j.net.2017.02.001
300. Vano E, Ohno K, Cousins C, Niwa O, Boice J (2011) Radiation risks and radiation protection training for healthcare professionals: iCRP and the Fukushima experience. J Radiol Prot 31(3):285–287. https://doi.org/10.1088/0952-4746/31/3/e03
301. Sasakawa Y, Kiikuni K, Kikuchi S, Niwa O, Yamashita S, Heymann DL, Mettler FA, Akashi M, Boice JD, Bouville A, Bromet EJ, Chumak V, Clement CH, Coleman CN, Cooper JR, Davis S, van Deventer TE, Gonzalez AJ, Gusev I, Homma T, Ivanov V, Kai M, Kamiya K, Kodama K, Lee J, Lochard J, Mabuchi K, Maekawa K, Menzel HG, Napier B, Okubo T, Sakai K, Schneider AB, Shima A, Takenoshita S, Thomas GA, Tronko MD, Wakeford R, Walker T, Weiss W, Wondergem J, Yonekura Y, Zeeb H, Int Expert Symposium F (2011) Conclusions and recommendations of the International Expert Symposium in Fukushima:

radiation and health risks. J Radiol Prot 31(4):381–384. https://doi.org/10.1088/0952-4746/31/4/e02
302. Suzuki T (2011) Deconstructing the zero-risk mindset: the lessons and future responsibilities for a post-Fukushima nuclear Japan. Bull At Sci 67(5):9–18. https://doi.org/10.1177/0096340211421477
303. Clement C, Niwa O, Van Deventer E (2012) International expert symposium in Fukushima: radiation and health risks. J Radiol Prot 32(1):E9–E10. https://doi.org/10.1088/0952-4746/32/1/e05
304. Cranga M, Chevalier-Jabet K, Marchetto C, Mun C (2012) Evaluations of MCCI risks for the Fukushima events; related IRSN R&D strategy on corium retention and coolability, pp 282–289
305. Hasegawa K (2012) Facing nuclear risks: lessons from the Fukushima Nuclear Disaster. Int J Jpn Sociol 21(1):84–91. https://doi.org/10.1111/j.1475-6781.2012.01164.x
306. Matsumoto K, Sakuma A, Ueda I, Nagao A, Takahashi Y (2016) Psychological trauma after the Great East Japan earthquake. Psychiatry Clin Neurosci 70(8):318–331. https://doi.org/10.1111/pcn.12403
307. Ng KH, Lean ML (2012) The Fukushima nuclear crisis reemphasizes the need for improved risk communication and better use of social media. Health Phys 103(3):307–310. https://doi.org/10.1097/HP.0b013e318257cfcb
308. Suzuki Y, Yabe H, Yasumura S, Ohira T, Niwa SI, Ohtsuru A, Mashiko H, Maeda M, Abe M, Mental Hlth Grp Fukushima Hlth M (2015) Psychological distress and the perception of radiation risks: the Fukushima health management survey. Bull World Health Organ 93(9):598–605. https://doi.org/10.2471/blt.14.146498
309. Han SJ (2017) Global risks and cosmopolitan citizens in east Asia: a look at the Fukushima disaster and nuclear power plant. Dev Soc 46(2):195–225. https://doi.org/10.21588/dns/2017.46.2.001
310. Juraku K (2016) Deficits of Japanese nuclear risk governance remaining after the fukushima accident: case of contaminated water management. In: Earthquakes, tsunamis and nuclear risks: prediction and assessment beyond the Fukushima accident. Springer Japan, Tokyo, pp 157–169. https://doi.org/10.1007/978-4-431-55822-4_12
311. Ronde P, Hussler C (2012) Living in the vicinity of nuclear power stations: A specific perception and acceptance of related risks? CyberGeo 2012. https://doi.org/10.4000/cybergeo.25581
312. Lynas M (2012) Radiation and risk: fears, phobia and Fukushima. World Nuclear Association, pp 126–138
313. Groen RS, Bae JY, Lim KJ (2012) Fear of the unknown: ionizing radiation exposure during pregnancy. Am J Obstet Gynecol 206(6):456–462. https://doi.org/10.1016/j.ajog.2011.12.001
314. Higashi T, Kudo T, Kinuya S (2012) Radioactive iodine (I-131) therapy for differentiated thyroid cancer in Japan: current issues with historical review and future perspective. Ann Nucl Med 26(2):99–112. https://doi.org/10.1007/s12149-011-0553-4
315. Gulland A (2013) Global cancer risk from Fukushima is low, says WHO. BMJ-Br Med J 346:1. https://doi.org/10.1136/bmj.f1390
316. Hiranuma Y (2016) Misrepresented risk of thyroid cancer in Fukushima. Lancet Diabetes Endocrinol 4(12):970. https://doi.org/10.1016/s2213-8587(16)30322-9
317. Murakami M, Tsubokura M, Ono K, Nomura S, Oikawa T (2017) Additional risk of diabetes exceeds the increased risk of cancer caused by radiation exposure after the Fukushima disaster. PLoS ONE 12(9):14. https://doi.org/10.1371/journal.pone.0185259
318. Shimura H, Ohana N (2013) Current situation and the role of department of clinical laboratory medicine on the Fukushima Health Management Survey Project for risk of thyroid cancer. Rinsho Byori 61(12):1166–1171
319. Takamura N, Orita M, Saenko V, Yamashita S, Nagataki S, Demidchik Y (2016) Radiation and risk of thyroid cancer: Fukushima and chernobyl (vol 4, p 647. Lancet Diabetes Endocrinol 4(10):E10–E10. https://doi.org/10.1016/s2213-8587(16)30197-8
320. Tanooka H (2015) Dose rate problems in extrapolation of hiroshima-nagasaki atomic bomb data to estimation of cancer risk of elevated environmental radiation in Fukushima. In: Fukushima nuclear accident: global implications, long-term health effects and ecological consequences. Nova Science Publishers, Inc., pp 101–113
321. Walsh L, Zhang W, Shore RE, Auvinen A, Laurier D, Wakeford R, Jacob P, Gent N, Anspaugh LR, Schuz J, Kesminiene A, van Deventer E, Tritscher A, Perez MDR (2014) A framework for estimating radiation-related cancer risks in Japan from the 2011 Fukushima nuclear accident. Radiat Res 182(5):556–572. https://doi.org/10.1667/rr13779.1
322. Yamashita S, Suzuki S (2013) Risk of thyroid cancer after the Fukushima nuclear power plant accident. Respir Invest 51(3):128–133. https://doi.org/10.1016/j.resinv.2013.05.007
323. Yamashita S, Takamura N, Ohtsuru A, Suzuki S (2016) Radiation exposure and thyroid cancer risk after the Fukushima nuclear power plant accident in comparison with the chernobyl accident. Radiat Prot Dosimet 171(1):41–46. https://doi.org/10.1093/rpd/ncw189
324. Gauthier-Lafaye F, Holliger P, Blanc PL (1996) Natural fission reactors in the Franceville basin, Gabon: a review of the conditions and results of a "critical event" in a geologic system. Geochim Cosmochim Acta 60(23):4831–4852. https://doi.org/10.1016/S0016-7037(96)00245-1
325. Hidaka A, Ishikawa J (2014) Quantities of I-131 and Cs-137 in accumulated water in the basements of reactor buildings in process of core cooling at Fukushima Daiichi nuclear power plants accident and its influence on late phase source terms. J Nucl Sci Technol 51(4):413–424. https://doi.org/10.1080/00223131.2014.881725
326. Kaiser JC (2014) Empirical risk analysis of severe reactor accidents in nuclear power plants after Fukushima (vol 2012, 384987, 2012). Sci Technol Nucl Install. https://doi.org/10.1155/2014/469890
327. Kataoka I (2013) Review of thermal-hydraulic researches in severe accidents in light water reactors. J Nucl Sci Technol 50(1):1–14. https://doi.org/10.1080/00223131.2013.750797
328. Kato H, Onda Y, Gomi T (2012) Interception of the Fukushima reactor accident-derived137Cs, 134Cs and 131I by coniferous forest canopies. Geophys Res Lett 39(20):L20403. https://doi.org/10.1029/2012GL052928
329. Liu ZT, Fan JH (2014) Technology readiness assessment of small modular reactor (SMR) designs. Prog Nucl Energy 70:20–28. https://doi.org/10.1016/j.pnucene.2013.07.005
330. Nagakawa Y, Sotodate T, Kinjo Y, Suzuki T (2015) One-year time variations of anthropogenic radionuclides in aerosols in Tokyo after the Fukushima Dai-ichi nuclear power plant reactor failures. J Nucl Sci Technol 52(6):784–791. https://doi.org/10.1080/00223131.2014.985279
331. Nagataki S, Takamura N (2014) A review of the Fukushima nuclear reactor accident: radiation effects on the thyroid and strategies for prevention. Curr Opin Endocrinol Diabetes Obes 21(5):384–393. https://doi.org/10.1097/med.0000000000000098
332. Park KH, Kang TW, Kim WJ, Park JW (2013) Cs-134 and Cs-137 radioactivity in soil and moss samples of Jeju Island after Fukushima nuclear reactor accident. Appl Radiat Isotop 81:379–382. https://doi.org/10.1016/j.apradiso.2013.03.066
333. Ritchie LT, Brown WD, Wayland JR (1980) Impact of rainstorm and runoff modeling on predicted consequences of atmospheric releases from nuclear reactor accidents (No. NUREG/CR--1244) Sandia Labs

334. Takeya Y, Miwa S, Hibiki T, Mori M (2015) Application of steam injector to improved safety of light water reactors. Prog Nucl Energy 78:80–100. https://doi.org/10.1016/j.pnucene.2014.07.045
335. Wang W (2013) Risk reporting in the Chinese news media in response to radiation threat from the Fukushima nuclear reactor crisis. https://doi.org/10.1115/icem2013-96360
336. Wang W, ASME (2013) Risk reporting in the chinese news media in response to radiation threat from the Fukushima nuclear reactor crisis. In: ASME 2013 15th international conference on environmental remediation and radioactive waste management, vol 2: Facility Decontamination and Decommissioning; Environmental Remediation; Environmental Management/Public Involvement/Crosscutting Issues/Global Partnering. American Society Mechanical Engineers, New York. https://doi.org/10.1115/icem2013-96360
337. Wang Y, Ma JE, Fang YT (2016) Generation III pressurized water reactors and China's nuclear power. J Zhejiang Univ Sci A 17(11):911–922. https://doi.org/10.1631/jzus.A1600035
338. Wendel CCS, Lind OC, Fifield LK, Tims SG, Salbu B, Oughton DH (2017) No Fukushima Dai-ichi derived plutonium signal in marine sediments collected 1.5–57 km from the reactors. Appl Radiat Isotop 129:180–184. https://doi.org/10.1016/j.apradiso.2017.08.015
339. Xing J, Song DY, Wu YX (2016) HPR1000: advanced pressurized water reactor with active and passive safety. Engineering 2(1):79–87. https://doi.org/10.1016/j.eng.2016.01.017
340. Yadav MK, Khandekar S, Sharma PK (2016) An integrated approach to steam condensation studies inside reactor containments: a review. Nucl Eng Des 300:181–209. https://doi.org/10.1016/j.nucengdes.2016.01.004
341. Eddy C, Sase E (2015) Implications of the Fukushima nuclear disaster: man-made hazards, vulnerability factors, and risk to environmental health. J Environ Health 78(1):26–32
342. Goto A, Rudd RE, Lai AY, Yoshida K, Suzuki Y, Halstead DD, Yoshida-Komiya H, Reich MR (2014) Leveraging public health nurses for disaster risk communication in Fukushima City: a qualitative analysis of nurses' written records of parenting counseling and peer discussions. BMC Health Serv Res. https://doi.org/10.1186/1472-6963-14-129
343. Ho JC, Lee CTP, Kao SF, Chen RY, Ieong MCF, Chang HL, Hsieh WH, Tzeng CC, Lu CF, Lin SL, Chang PW (2014) Perceived environmental and health risks of nuclear energy in Taiwan after Fukushima nuclear disaster. Environ Int 73:295–303. https://doi.org/10.1016/j.envint.2014.08.007
344. Inamasu T (2013) Fukushima radiation health risk management. Nucl Plant J 31(4):42–45
345. Inamasu T, Schonfeld SJ, Abe M, Bidstrup PE, Deltour I, Ishida T, Ishikawa T, Kesminiene A, Ohira T, Ohto H, Suzuki S, Thierry-Chef I, Yabe H, Yasumura S, Schuz J, Yamashita S (2015) Meeting report: suggestions for studies on future health risks following the Fukushima accident. Environ Health 14:4. https://doi.org/10.1186/s12940-015-0013-z
346. Maeno R, Pearse W, Sendall MC (2014) The Fukushima nuclear power plant disaster and perceptions of health risk communication: a case study. J Health Saf Environ 30(1):1–15
347. Matsuda N, Morita N, Miura M (2014) Assessment and control of health risk caused by the radiological accident at the TEPCO Fukushima Daiichi nuclear power plant. Yakugaku Zasshi 134(2):135–142. https://doi.org/10.1248/yakushi.13-00227-1
348. Miura I, Nagai M, Maeda M, Harigane M, Fujii S, Oe M, Yabe H, Suzuki Y, Takahashi H, Ohira T, Yasumura S, Abe M (2017) Perception of radiation risk as a predictor of mid-term mental health after a nuclear disaster: the Fukushima Health Management Survey. Int J Env Res Public Health 14(9):13. https://doi.org/10.3390/ijerph14091067
349. Morioka R (2014) Gender difference in the health risk perception of radiation from Fukushima in Japan: the role of hegemonic masculinity. Soc Sci Med 107:105–112. https://doi.org/10.1016/j.socscimed.2014.02.014
350. Murakami M, Oki T (2015) Estimated dietary intake of radionuclides and health risks for the citizens of Fukushima City, Tokyo, and Osaka after the 2011 nuclear accident (vol 9, e112791, 2014). PLoS ONE 10(8):3. https://doi.org/10.1371/journal.pone.0136223
351. Ohira T, Hosoya M, Yasumura S, Satoh H, Suzuki H, Sakai A, Ohtsuru A, Kawasaki Y, Takahashi A, Ozasa K, Kobashi G, Hashimoto S, Kamiya K, Yamashita S, Abe M, Fukushima Hlth Management Survey G (2016) Evacuation and risk of hypertension after the Great East Japan Earthquake: the Fukushima Health Management Survey. Hypertension 68(3):558–564. https://doi.org/10.1161/hypertensionaha.116.07499
352. Ohira T, Nakano H, Nagai M, Yumiya Y, Zhang W, Uemura M, Sakai A, Hashimoto S (2017) Changes in cardiovascular risk factors after the Great East Japan Earthquake: a review of the comprehensive health check in the Fukushima Health Management Survey. Asia-Pac J Public Health 29(2 suppl):47S–55S. https://doi.org/10.1177/1010539517695436
353. Okamoto T (2012) The front line management of health risks from Fukushima nuclear power plant disaster. Nihon Geka Gakkai Zasshi 113(3):308
354. Orita M, Hayashida N, Nakayama Y, Shinkawa T, Urata H, Fukushima Y, Endo Y, Yamashita S, Takamura N (2015) Bipolarization of risk perception about the health effects of radiation in residents after the accident at Fukushima nuclear power plant. PLoS ONE 10(6):9. https://doi.org/10.1371/journal.pone.0129227
355. Satoh H, Ohira T, Nagai M, Hosoya M, Sakai A, Yasumura S, Ohtsuru A, Kawasaki Y, Suzuki H, Takahashi A, Sugiura Y, Shishido H, Hayashi Y, Takahashi H, Kobashi G, Ozasa K, Hashimoto S, Ohto H, Abe M, Kamiya K (2017) Evacuation is a risk factor for diabetes development among evacuees of the Great East Japan earthquake: a 4-year follow-up of the Fukushima Health Management Survey. Diabetes Metab 1:1. https://doi.org/10.1016/j.diabet.2017.09.005
356. Shimura T, Yamaguchi I, Terada H, Robert Svendsen E, Kunugita N (2014) Public health activities for mitigation of radiation exposures and risk communication challenges after the Fukushima nuclear accident. J Radiat Res 56(3):422–429. https://doi.org/10.1093/jrr/rrv013
357. Suzuki K, Yamashita S (2015) Perspective: health-risk implications of the fukushima nuclear power plant accident. In: Fukushima nuclear accident: global implications, long-term health effects and ecological consequences. Nova Science Publishers, Inc., Hauppauge, pp 1–25
358. Takada J (2013) Low dose radiation and no health risk in Fukushima in contrast to Chernobyl. Genes Environ 35(3):69–72. https://doi.org/10.3123/jemsge.2013.005
359. Vyncke B, Perko T, Van Gorp B (2017) Information sources as explanatory variables for the Belgian health-related risk perception of the Fukushima Nuclear Accident. Risk Anal 37(3):570–582. https://doi.org/10.1111/risa.12618
360. Yamashita S (2012) Lessons learnt from chernobyl and health risk management after Fukushima nuclear disaster. Nihon Geka Gakkai Zasshi 113(3):309–313
361. Yamashita S (2014) Tenth warren k. sinclair keynote address-the fukushima nuclear power plant accident and comprehensive health risk management. Health Phys 106(2):166–180. https://doi.org/10.1097/hp.0000000000000007
362. Yamashita S (2014) Fukushima nuclear power plant accident and comprehensive health risk management—global

radiocontamination and information disaster. Trop Med Health 42(2):93–107. https://doi.org/10.2149/tmh.2014-S14
363. Yamashita S, Radiation Med Sci Ctr Fukushima H (2016) Comprehensive health risk management after the Fukushima nuclear power plant accident. Clin Oncol 28(4):255–262. https://doi.org/10.1016/j.clon.2016.01.001
364. Murakami M, Tsubokura M (2017) Evaluating risk communication after the Fukushima disaster based on nudge theory. Asia Pac J Public Health 29:193S–200S. https://doi.org/10.1177/1010539517691338
365. Bottino PJ, Sparrow AH (1973) Influence of seasonal-variation on survival and yield of lettuce irradiated with constant rate, fallout decay or buildup and fallout decay simulation treatments. Radiat Bot 13(1):27–36. https://doi.org/10.1016/0033-7560(73)90031-8
366. Sorensen B (1975) Computer-simulation of I-131 transfer from fallout to man. Water Air Soil Pollut 4(1):65–87. https://doi.org/10.1007/bf01794131
367. Yoneda M, Morisawa S, Sasaki T, Inoue Y (1993) Dynamic behavior of fallout cs-137 in paddy field and its accumulation in rice—evaluation by applying conditional simulation. J At Energy Soc Jpn 35(7):649–661. https://doi.org/10.3327/jaesj.35.649
368. Kato M, Okada Y, Hirai S, Minai Y, Saito S, Shibukawa M (2016) Comparative analysis of distributions of radioactive cesium and potassium and stable cesium, potassium, and strontium in brown rice grains contaminated with radioactive materials released by the Fukushima Daiichi nuclear power plant accident. J Radioanal Nucl Chem 310(1):247–252. https://doi.org/10.1007/s10967-016-4824-3
369. Mosca R, Giribone P, Bruzzone AG (1994) Automated modeling of chemical fallout through simulation. In: Simulation for emergency management: proceedings of the 1994 simulation multiconference. Soc Computer Simulation International, San Diego
370. Bruzzone AG, Giribone P, Mosca R (1996) Simulation of hazardous material fallout for emergency management during accidents. SIMULATION 66(6):343–356. https://doi.org/10.1177/003754979606600603
371. Ichikawa S, Yamamoto I, Murai M, Watanabe K (1996) Fallout decay simulation experiments with the stamen hairs of stable and mutable Tradescantia clones. Environ Exp Bot 36(2):173–184. https://doi.org/10.1016/0098-8472(96)01006-4
372. Macacini JF, Fernandes EAD, Taddei MHT (2002) Translocation studies of Cs-137 and Sr-90 in bean plants (*Phaseolus vulgaris*): simulation of fallout. Environ Pollut 120(1):151–155. https://doi.org/10.1016/s0269-7491(02)00140-9
373. Macedonio G, Costa A, Folch A (2008) Ash fallout scenarios at Vesuvius: numerical simulations and implications for hazard assessment. J Volcanol Geotherm Res 178(3):366–377. https://doi.org/10.1016/j.jvolgeores.2008.08.014
374. Inagaki K, Hijikata T, Tsukada T, Koyama T, Ishikawa K, Ono S, Suzuki S (2014) Early construction and operation of the highly contaminated water treatment system in Fukushima Daiichi Nuclear Power Station (III)—a unique simulation code to evaluate time-dependent Cs adsorption/desorption behavior in column system. J Nucl Sci Technol 51(7–8):906–915. https://doi.org/10.1080/00223131.2014.921580
375. Nakayama H, Takemi T, Nagai H (2015) Large-eddy simulation of turbulent winds during the Fukushima Daiichi nuclear power plant accident by coupling with a meso-scale meteorological simulation model. Adv Sci Res 12:127–133. https://doi.org/10.5194/asr-12-127-2015
376. Mori K, Tada K, Tawara Y, Ohno K, Asami M, Kosaka K, Tosaka H (2015) Integrated watershed modeling for simulation of spatiotemporal redistribution of post-fallout radionuclides: application in radiocesium fate and transport processes derived from the Fukushima accidents. Environ Model Softw 72:126–146. https://doi.org/10.1016/j.envsoft.2015.06.012
377. Kim E, Tani K, Kunishima N, Kurihara O, Sakai K, Akashi M (2016) Estimation of early internal doses to fukushima residents after the nuclear disaster based on the atmospheric dispersion simulation. Radiat Prot Dosimet 171(3):398–404. https://doi.org/10.1093/rpd/ncv385
378. Wei LZ, Kinouchi T, Velleux ML, Omata T, Takahashi K, Araya M (2017) Soil erosion and transport simulation and critical erosion area identification in a headwater catchment contaminated by the Fukushima nuclear accident. J Hydro-environ Res 17:18–29. https://doi.org/10.1016/j.jher.2017.09.003
379. Lee HJ, Jo HY, Nam KP, Lee KH, Kim CH (2017) Measurement, simulation, and meteorological interpretation of medium-range transport of radionuclides to Korea during the Fukushima Daiichi nuclear accident. Ann Nucl Energy 103:412–423. https://doi.org/10.1016/j.anucene.2017.01.037
380. Nagai H, Terada H, Tsuduki K, Katata G, Ota M, Furuno A, Akari S (2017) Updating source term and atmospheric dispersion simulations for the dose reconstruction in Fukushima Daiichi Nuclear Power Station Accident. In: Malvagi F, Malouch F, Diop CMB, Miss J, Trama JC (eds) Icrs-13 & Rpsd-2016, 13th International conference on radiation shielding & 19th Topical meeting of the radiation protection and shielding division of the American Nuclear Society 2016, vol 153. EPJ Web of Conferences. E D P Sciences, Cedex A. https://doi.org/10.1051/epjconf/201715308012
381. Prants SV, Budyansky MV, Uleysky MY (2017) Lagrangian simulation and tracking of the mesoscale eddies contaminated by Fukushima-derived radionuclides. Ocean Sci 13(3):453–463. https://doi.org/10.5194/os-13-453-2017
382. Takahashi H, Takahashi K, Shimura H, Yasumura S, Suzuki S, Ohtsuru A, Midorikawa S, Ohira T, Ohto H, Yamashita S, Kamiya K (2017) Simulation of expected childhood and adolescent thyroid cancer cases in Japan using a cancer-progression model based on the National Cancer Registry Application to the first-round thyroid examination of the Fukushima Health Management Survey. Medicine (Baltimore) 96(48):9. https://doi.org/10.1097/md.0000000000008631
383. Koh HL, Teh SY, Abas MRC (2014) Post Fukushima tsunami simulations for Malaysian coasts. In: Dass SC, Guan BH, Bhat AH, Faye I, Soleimani H, Yahya N (eds) 3rd International conference on fundamental and applied sciences, vol 1621. AIP conference proceedings. American Institute of Physics, Melville, pp 373–378. https://doi.org/10.1063/1.4898494
384. Leibowicz BD (2014) Evaluation of post-Fukushima Japanese electricity strategies: a stochastic simulation model. Int J Energy Res 38(12):1578–1598. https://doi.org/10.1002/er.3181
385. Misumi K, Tsumune D, Tsubono T, Tateda Y, Aoyama M, Kobayashi T, Hirose K (2014) Factors controlling the spatiotemporal variation of Cs-137 in seabed sediment off the Fukushima coast: implications from numerical simulations. J Environ Radioact 136:218–228. https://doi.org/10.1016/j.jenvrad.2014.06.004
386. Prants SV, Budyansky MV, Uleysky MY (2014) Lagrangian study of surface transport in the Kuroshio Extension area based on simulation of propagation of Fukushima-derived radionuclides. Nonlinear Process Geophys 21(1):279–289. https://doi.org/10.5194/npg-21-279-2014
387. Nakajima H, Yamaguchi Y, Yoshimura T, Fukumoto M, Todo T (2015) Fukushima simulation experiment: assessing the effects of chronic low-dose-rate internal Cs-137 radiation exposure on litter size, sex ratio, and biokinetics in mice. J Radiat Res 56:I29–I35. https://doi.org/10.1093/jrr/rrv079
388. Sekiyama TT, Kunii M, Kajino M, Shimbori T (2015) Horizontal resolution dependence of atmospheric simulations of the Fukushima nuclear accident using 15-km, 3-km, and 500-m grid

models. J Meteorol Soc Jpn 93(1):49–64. https://doi.org/10.2151/jmsj.2015-002
389. Tateda Y, Tsumune D, Tsubono T, Misumi K, Yamada M, Kanda J, Ishimaru T (2016) Status of Cs-137 contamination in marine biota along the Pacific coast of eastern Japan derived from a dynamic biological model two years simulation following the Fukushima accident. J Environ Radioact 151:495–501. https://doi.org/10.1016/j.jenvrad.2015.05.013
390. Kawamura H, Kobayashi T, Furuno A, Usui N, Kamachi M (2014) Numerical simulation on the long-term variation of radioactive cesium concentration in the North Pacific due to the Fukushima disaster. J Environ Radioact 136:64–75. https://doi.org/10.1016/j.jenvrad.2014.05.005
391. Saito T, Kurihara Y, Koike Y, Tanihata I, Fujiwara M, Sakaguchi H, Shinohara A, Yamamoto H (2015) Altitude distribution of radioactive cesium at Fuji volcano caused by Fukushima Daiichi Nuclear Power Station accident. J Radioanal Nucl Chem 303(2):1613–1615. https://doi.org/10.1007/s10967-014-3753-2
392. Nakano M, Povinec PP (2012) Long-term simulations of the Cs-137 dispersion from the Fukushima accident in the world ocean. J Environ Radioact 111:109–115. https://doi.org/10.1016/j.jenvrad.2011.12.001
393. Kobayashi T, Nagai H, Chino M, Kawamura H (2013) Source term estimation of atmospheric release due to the Fukushima Dai-ichi nuclear power plant accident by atmospheric and oceanic dispersion simulations. J Nucl Sci Technol 50(3):255–264. https://doi.org/10.1080/00223131.2013.772449
394. Tateda Y, Tsumune D, Tsubono T (2013) Simulation of radioactive cesium transfer in the southern Fukushima coastal biota using a dynamic food chain transfer model. J Environ Radioact 124:1–12. https://doi.org/10.1016/j.jenvrad.2013.03.007
395. Tsumune D, Tsubono T, Aoyama M, Uematsu M, Misumi K, Maeda Y, Yoshida Y, Hayami H (2013) One-year, regional-scale simulation of Cs-137 radioactivity in the ocean following the Fukushima Dai-ichi nuclear power plant accident. Biogeosciences 10(8):5601–5617. https://doi.org/10.5194/bg-10-5601-2013
396. Draxler R, Arnold D, Chino M, Galmarini S, Hort M, Jones A, Leadbetter S, Malo A, Maurer C, Rolph G, Saito K, Servranckx R, Shimbori T, Solazzo E, Wotawa G (2015) World Meteorological Organization's model simulations of the radionuclide dispersion and deposition from the Fukushima Daiichi nuclear power plant accident. J Environ Radioact 139:172–184. https://doi.org/10.1016/j.jenvrad.2013.09.014
397. Srinivas CV, Venkatesan R, Baskaran R, Rajagopal V, Venkatraman B (2012) Regional scale atmospheric dispersion simulation of accidental releases of radionuclides from Fukushima Dai-ichi reactor. Atmos Environ 61:66–84. https://doi.org/10.1016/j.atmosenv.2012.06.082
398. Cardoni J, Gauntt R, Kalinich D, Phillips J (2014) Melcor simulations of the severe accident at Fukushima Daiichi unit 3. Nucl Technol 186(2):179–197. https://doi.org/10.13182/nt13-41
399. Fei JF, Wang PF, Cheng XP, Huang XG, Wang YB (2014) A regional simulation study on dispersion of nuclear pollution from the damaged Fukushima nuclear power plant. Sci China-Earth Sci 57(7):1513–1524. https://doi.org/10.1007/s11430-013-4811-2
400. Gauntt R, Kalinich D, Cardoni J, Phillips J (2014) Melcor simulations of the severe accident at the Fukushima Daiichi Unit 1 reactor. Nucl Technol 186(2):161–178. https://doi.org/10.13182/nt13-59
401. Bonneville H, Luciani A (2014) Simulation of the core degradation phase of the Fukushima accidents using the ASTEC code. Nucl Eng Des 272:261–272. https://doi.org/10.1016/j.nucengdes.2013.06.043
402. Bocanegra R, Di Marcello V, Sanchez V, Jimenez G, Asme (2016) Fukushima unit 2 accident simulation with melcor 2.1. In: Proceedings of the 24th international conference on nuclear engineering, 2016, vol 5. American Society of Mechanical Engineers, New York
403. Bonneville H, Carenini L, Barrachin M (2016) Core Melt Composition at Fukushima Daiichi: results of Transient Simulations with ASTEC. Nucl Technol 196(3):489–498. https://doi.org/10.13182/nt16-27
404. Chiang Y, Chen SW, Wang JR, Wang TY, Chen HC, Hsu WS, Chiang SC, Shih C (2017) Code crosswalk of Fukushima-like simulations for Chinshan BWR/4 NPP using MELCOR2.1/SNAP, TRACE/SNAP, PCTRAN and MAAP5.03. Nucl Eng Des 325:12–24. https://doi.org/10.1016/j.nucengdes.2017.09.023
405. Xiao JJ, Breitung W, Kuznetsov M, Zhang H, Travis JR, Redlinger R, Jordan T (2017) GASFLOW-MPI: a new 3-D parallel all-speed CFD code for turbulent dispersion and combustion simulations part II: first analysis of the hydrogen explosion in Fukushima Daiichi Unit 1. Int J Hydrogen Energy 42(12):8369–8381. https://doi.org/10.1016/j.ijhydene.2017.01.219
406. The long shadow from Chernobyl (1986). Nature 321(6066):099. https://doi.org/10.1038/321099a0
407. Weast RC, Selby S (1971) Handbook of chemistry and physics, The Chemical Rubber Co. 77
408. IAEA FNAL (05.11.2017) IAEA, Fukushima Nuclear Accident Log. https://www.iaea.org/news/2011/fukushimafull.html
409. Gauss CF (1809) Theoria motus corporum coelestum. Werke
410. Bayazıt M, Oğuz EBY (2005) Mühendisler için istatistik. Birsen Yayınevi
411. Cramér H (2004) Random variables and probability distributions, vol 36. Cambridge University Press, Cambridge
412. Evans M, Hastings NAJ, Peacock JB (1993) Statistical distributions. Wiley, New York
413. Wolberg J (2006) Data analysis using the method of least squares: extracting the most information from experiments. Springer, Berlin. https://doi.org/10.1007/3-540-31720-1
414. Şen Z (1999) Simple risk calculations in dependent hydrological series. Hydrol Sci J 44(6):871–878
415. Şen Z (1976) Wet and dry periods of annual flow series. J Hydraul Div 102(10):1503–1514
416. Külahci F, Şen Z (2009) Risk assessment of distribution coefficient from 137Cs measurements. Environ Monit Assess 149(1–4):363–370. https://doi.org/10.1007/s10661-008-0209-6
417. Embrechts P, Klüppelberg C, Mikosch T (2013) Modelling extremal events: for insurance and finance, vol 33. Springer Science & Business Media, Berlin
418. Leadbetter MR, Lindgren G, Rootzén H (2012) Extremes and related properties of random sequences and processes. Springer Science & Business Media, Berlin
419. Resnick S (2008) Extreme values, regular variation and point processes. Springer series in operations research and financial engineering. Springer, Berlin
420. Coles S, Bawa J, Trenner L, Dorazio P (2001) An introduction to statistical modeling of extreme values, vol 208. Springer, Berlin
421. Cressie N (1991) Statistics for spatial data. Wiley, New York
422. Davis JC, Sampson RJ (2002) Statistics and data analysis in geology, vol 646. Wiley, New York
423. de Lavenne A, Skøien JO, Cudennec C, Curie F, Moatar F (2016) Transferring measured discharge time series: large-scale comparison of Top-kriging to geomorphology-based inverse modeling. Water Resour Res 52(7):5555–5576. https://doi.org/10.1002/2016WR018716